MALARIA

Adjunctive ruxolitinib attenuates inflammation and enhances immunity in volunteers experimentally infected with *Plasmodium falciparum*

Rebecca Webster[1]†, Damian A. Oyong[2]†, Stacey Llewellyn[1,3], Azrin N. Abd-Rahman[1], Adam J. Potter[1], Reena Mukhiya[2,4], Nischal Sahai[5], Indika Leelasena[5], Eniko Ujvary[5], Sue Mathison[5], Dean W. Andrew[1], Luzia Bukali[1], Fabian de Labastida Rivera[1], Jessica Engel[1], Megan S. F. Soon[2], Teija Frame[1], Julianne Hamelink[2,6], Mayimuna Nalubega[2,6], Nicholas L. Dooley[2], Jessica R. Loughland[2], Tran Nguyen[7], Yael Rosenberg-Hasson[7], Sofia Maysel-Auslender[7], Natalia Sigal[7], Kira Foygel[7], Jeremy Gower[1], Jenny Peters[1], Ria Woo[1], Fiona Amante[1], Timothy N. C. Wells[8], Stephan Chalon[8], Joerg J. Moehrle[8,9,10], James S. McCarthy[1,11], Geoffrey W. Birrell[12], Michael D. Edstein[12], Michael Leipold[7], Gerlinde Obermoser[7], Holden Maecker[7], Christian R. Engwerda[1]*‡, Bridget E. Barber[1,5,13,14]*‡, Michelle J. Boyle[2,4,6]*‡

Inhibiting the inflammatory response to malaria offers a promising strategy to improve clinical outcomes and overcome immunoregulatory barriers that hinder development of antiparasitic immunity. We conducted a double-blind, randomized, placebo-controlled trial assessing whether ruxolitinib, a Janus-activated kinase (JAK) 1/2 inhibitor, can reduce inflammatory responses and enhance antiparasitic immunity in malaria-naïve volunteers inoculated with blood-stage *Plasmodium falciparum*. Twenty participants were inoculated and, on day 8, randomized to receive artemether-lumefantrine with either ruxolitinib or placebo. Ninety days later, participants underwent a second inoculation. Ruxolitinib was safe and well tolerated; moreover, it attenuated inflammatory responses to the initial infection, with reduced posttreatment increases in C-reactive protein and markers of disease severity, including angiopoietin-2 and intercellular adhesion molecule-1. Ruxolitinib also enhanced immune memory after the second infection, with elevated human leukocyte antigen–DRA and 4-1BB, consistent with increased T cell activation. These data support the further evaluation of ruxolitinib as an adjunctive treatment to improve clinical outcomes and boost antiparasitic immunity in clinical malaria.

INTRODUCTION

Malaria remains a major public health challenge, with 263 million cases and 597,000 deaths reported globally in 2023, the majority from *Plasmodium falciparum* (*1*). Current efforts to control malaria have stalled, and case-fatality rates from severe malaria remain high despite the use of highly effective antiparasitic drug treatments (*2*). Although the recent introduction of two malaria vaccines offers promise, the efficacy and duration of protection are suboptimal, particularly in populations with the highest malaria burdens (*3*–*5*). Thus, additional strategies are urgently needed to enhance the efficacy of current drug and vaccine approaches.

Emerging evidence suggests that development of protective immunity after clinical malaria or vaccination is impeded by malaria-induced immunoregulatory pathways (*6*). These pathways are driven by type I interferons (IFNs) that are produced early in malaria infection and result in the development of key regulatory responses, including the development of interleukin-10 (IL-10)–producing type I regulatory $CD4^+$ T ($T_{reg}1$) cells (*7*–*10*). Although these immunoregulatory mechanisms may protect against disease mediated by the inflammatory response (*11*, *12*), they may also impede the development of protective antiparasitic immunity after natural infection, vaccination, or antiparasitic drug treatment (*6*, *13*).

Type I IFNs signal through the recruitment of Janus-activated kinases (JAK) 1 and 2 to the cytosolic domains of the type I IFN receptor, leading to phosphorylation of signal transducer and activator of transcription (STAT) 1, 2, and 3 (*14*). This signaling cascade is essential for promoting the differentiation of immunoregulatory cells, including their production of IL-10 and expression of co-inhibitory receptors (*9*, *10*). Thus, targeting type-1 IFN signaling offers a promising strategy to enhance antiparasitic immunity after malaria treatment or vaccination. Ruxolitinib is an oral JAK1/2 inhibitor approved for treating adults with myelofibrosis, polycythemia vera, and steroid-refractory graft-versus-host disease and has been used in children with type-1 interferonopathy (*15*). We recently demonstrated that ruxolitinib suppressed type-1 IFN signaling and enhanced antiparasitic $CD4^+$ T cell responses when administered with antiparasitic drugs in a preclinical model of visceral

[1]QIMR Berghofer, Brisbane, QLD 4006, Australia. [2]Burnet Institute, Melbourne, VIC 3004, Australia. [3]George Institute for Global Health, NSW 2031, Australia. [4]Griffith University, Brisbane, QLD 4101, Australia. [5]University of Sunshine Coast Clinical Trials, Brisbane, QLD 4101, Australia. [6]University of Queensland, Brisbane, QLD 4000, Australia. [7]Stanford University, Stanford, CA 94305, USA. [8]Medicines for Malaria Venture, Geneva 1215, Switzerland. [9]University of Basel, Basel 4056, Switzerland. [10]Swiss Tropical and Public Health Institute, Allschwil 4123, Switzerland. [11]Department of Infectious Diseases, University of Melbourne Peter Doherty Institute for Infection and Immunity, Melbourne, VIC 3000, Australia. [12]Australian Defence Force Malaria and Infectious Disease Institute, Brisbane, QLD 4053, Australia. [13]Royal Brisbane and Women's Hospital, Brisbane, QLD 4029, Australia. [14]Menzies School of Health Research, Darwin, NT 0810, Australia.
†These authors contributed equally to this work.
*Corresponding author. Email: bridget.barber@qimrb.edu.au (B.E.B.); Christian.Engwerda@qimrb.edu.au (C.R.E.); Michelle.Boyle@burnet.edu.au (M.J.B.)
‡These authors contributed equally to this work.

leishmaniasis (*16*). We therefore hypothesized that ruxolitinib could enhance antiparasitic immunity when used as an adjunctive treatment for malaria. Although ruxolitinib has been shown to be safe and free of clinically relevant drug interactions when coadministered with the first-line antimalarial artemether-lumefantrine in healthy volunteers (*17*), its use in individuals with malaria has not been evaluated.

We conducted a double-blind, randomized, placebo-controlled trial to assess whether ruxolitinib can modulate host immune responses and enhance protective immunity when administered with artemether-lumefantrine in malaria-naïve volunteers experimentally infected with blood-stage *P. falciparum*. The primary end point was safety and tolerability. Secondary end points included the effects of ruxolitinib on STAT3 phosphorylation, antimalarial drug concentrations, parasite clearance dynamics, inflammatory and immune responses, and parasite growth after a second homologous *P. falciparum* infection.

RESULTS

Study overview and participants

The study was conducted from 9 June 2021 to 7 July 2023. Twenty malaria-naïve volunteers were enrolled across six cohorts (Fig. 1). Participants were between 18 and 55 years old; 11 were male (55%), and 17 (85%) self-selected their race as white (Table 1). On day 0, participants were intravenously inoculated with ~2800 viable *P. falciparum* 3D7–infected red blood cells (RBCs). Parasitemia was monitored daily by quantitative polymerase chain reaction (qPCR) targeting the *P. falciparum* 18*S* ribosomal RNA (rRNA) gene from day 4 (data file S1). On day 8 (cohorts 3 to 6) or 9 (cohorts 1 and 2), participants were randomized to receive 20 mg of ruxolitinib or placebo, administered 2 hours after artemether-lumefantrine. All study drugs were administered orally twice daily for 3 days, under observation by clinical staff. Participants were confined at the clinical trial site for 72 hours after the first dose and were followed up as outpatients until day 28. On day 90 ± 7, participants still available and eligible were inoculated again with the same dose of *P. falciparum* 3D7–infected RBCs and treated with artemether-lumefantrine when parasitemia reached >50,000 parasites/ml or earlier if other prespecified clinical criteria were met; participants were again monitored as outpatients for 28 days after administration of artemether-lumefantrine.

After the first inoculation, parasitemia progressed as expected, with no difference in pretreatment parasitemia between treatment groups [11,084 (range of 968 to 149,520) parasites/ml in the placebo group and 11,586 (range of 363 to 251,802) parasites/ml in the ruxolitinib group; Table 1]. All 20 participants received artemether-lumefantrine and at least one dose of ruxolitinib ($n = 11$) or placebo

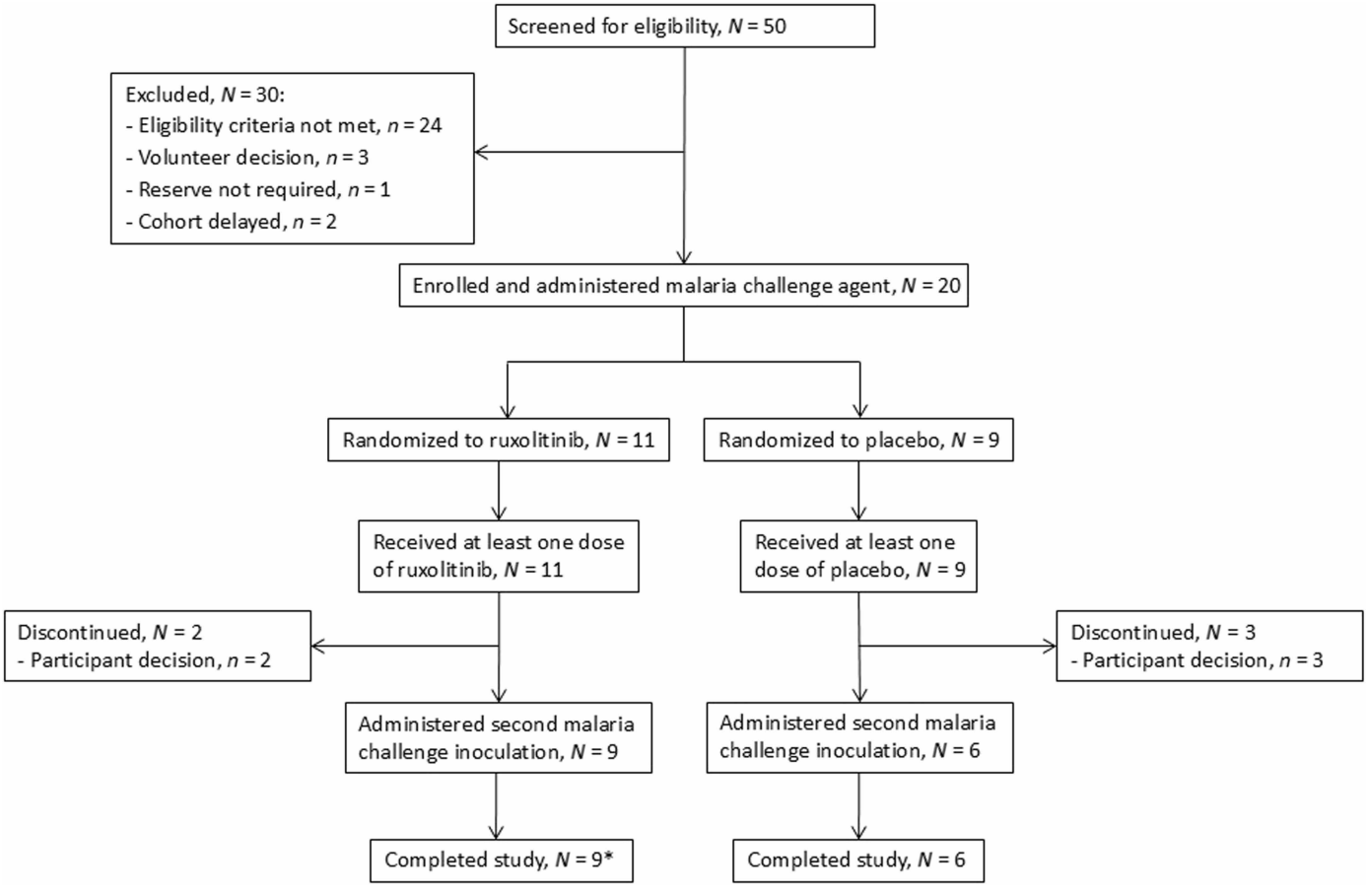

Fig. 1. Trial design. Twenty participants were inoculated with pRBCs and randomized on the day of dosing to receive artemether-lumefantrine with either ruxolitinib or placebo. All participants received at least one dose of ruxolitinib or placebo. Five participants, two in the ruxolitinib group and three in the placebo, discontinued voluntarily before administration of a second *P. falciparum* inoculation. *One participant in the ruxolitinib group tested positive for COVID-19 on day 6 after the second inoculation, necessitating early administration of artemether-lumefantrine.

Table 1. Participant characteristics and parasitemia at time of ruxolitinib or placebo administration. BMI, body mass index.

	All ($n = 20$)	Ruxolitinib ($n = 11$)	Placebo ($n = 9$)
Male sex, *n* (%)	11 (55)	7 (64)	4 (44)
Age, years (median, range)	33 (18–55)	38 (21–55)	27 (18–41)
BMI, kg/m^2 (median, range)	25 (20–31)	26 (21–31)	25 (20–29)
Race, *n* (%)			
White	17 (85)	8 (73)	9 (100)
Asian	1 (5)	1 (9)	0 (0)
Other*	2 (10)	2 (18)	0 (0)
Parasitemia, parasites/ml (geometric mean, range)	11,307 (363–251,802)	11,084 (968–149,520)	11,586 (363–251,802)

*One participant in the ruxolitinib group reported their race as Colombian and one as Iraqi.

($n = 9$) (Fig. 1). Three participants (two in the ruxolitinib group and one in the placebo group) had dosing discontinued after either two or three doses of ruxolitinib or placebo because of protocol-specified toxicity rules (detailed below).

Five participants (two in the ruxolitinib group and three in the placebo group) discontinued the study after the first inoculation phase (Fig. 1). One ruxolitinib-treated participant tested positive for COVID-19 on day 6 after the second inoculation, necessitating early administration of artemether-lumefantrine.

Safety

In the first inoculation phase, 124 adverse events (AEs) (data file S2) were reported after ruxolitinib/placebo [investigation medicinal product (IMP)] dosing, with 18 of 20 (90%) participants experiencing at least one AE (Table 2). After administration of IMP, participants in the ruxolitinib group experienced a median of four AEs [interquartile range (IQR) 1.5 to 6], compared with a median of seven AEs (IQR 2 to 14) in the placebo group ($P = 0.25$; table S1).

Most AEs were mild (86 of 124, 69%) or moderate (34 of 124, 27%) in severity, and most (84 of 124, 68%) were considered attributable to malaria (Table 2). There were no serious AEs. Thirty-five AEs were considered related to the IMP. Most of these were also considered related to malaria given that it was not possible to distinguish the causality. Headache was the most common IMP-related AE, with seven events reported in six participants (three participants per treatment group) (Table 3). The other IMP-related AEs were mostly laboratory abnormalities, including elevations in hepatic transaminase concentrations and decreases in white blood count, platelets, and hemoglobin. Most of the IMP-related AEs were mild or moderate in severity. There were three severe (grade 3) IMP-related AEs that resulted in discontinuation of IMP dosing. A concomitant elevation in alanine aminotransferase (ALT) (456 U/liter; normal range of 0 to 45 U/liter) and aspartate aminotransferase (360 U/liter; normal range of 0 to 41 U/liter) in one participant resulted in discontinuation of placebo after three doses. In another participant, a neutrophil count decrease (0.67×10^9/liter; normal range of 1.5×10^9 to 8.0×10^9/liter) resulted in discontinuation of ruxolitinib after two doses. In a third participant, dosing of ruxolitinib was ceased after three doses because of a platelet count decrease (81×10^9/liter; normal range 150×10^9 to 400×10^9/liter) that was of moderate severity (grade 2) but met a protocol-specified stopping criterion (platelet count drop of >50% from baseline).

Safety and tolerability of ruxolitinib after the first inoculation were further evaluated with a malaria clinical score calculated on the basis of number and severity of malaria-related symptoms and evaluated three times per day during confinement (table S2 and data file S3). The sum of the malaria clinical scores recorded at each time point during this posttreatment confinement period was associated with pretreatment parasitemia ($r = 0.71$, $P = 0.04$). The median sum was 7 [IQR 1 to 8, range 0 to 38] in the placebo group, compared to 2 (IQR 0 to 4, range 0 to 6) in the ruxolitinib group, although this difference was not statistically significant ($P = 0.16$; table S3).

After the second inoculation, 98 AEs were reported (data file S2). All participants experienced at least one AE (table S4). Participants in the ruxolitinib group experienced a median of five AEs before final artemether-lumefantrine treatment (IQR 1.8 to 7.8), similar to a median of 3.5 AEs (IQR 2.0 to 5.8) in the placebo group ($P = 0.60$; table S1).

Effect of ruxolitinib on artemether-lumefantrine and metabolite concentrations

Plasma concentrations of ruxolitinib, artemether, dihydroartemisinin (DHA), lumefantrine, and desbutyl-lumefantrine (DBL) were quantified by liquid chromatography–tandem mass spectrometry (LC-MS/MS) (data file S1). In the ruxolitinib group, ruxolitinib plasma concentration time profiles varied among participants (fig. S1A). Ruxolitinib was rapidly absorbed, with a mean maximum concentration (C_{max}) of 192 ng/ml (SD = 1.38) and a median time to C_{max} of 0.97 hours (range 0.93 to 2.98) after the first dose; the mean elimination half-life was short [2.4 hours (SD = 1.55)] (table S5).

Ruxolitinib reduced artemether absorption, with a mean artemether C_{max} after the first dose of 35.41 ng/ml (SD 1.77) in the ruxolitinib group compared with 67.80 ng/ml (SD 1.68) in the placebo group ($P = 0.028$; table S6 and fig. S1B). The mean artemether C_{max} was also significantly lower in the ruxolitinib group after the last dose on day 3 ($P = 0.019$). The artemether area under the concentration-time curve ($AUC_{0\text{-last}}$) was lower in the ruxolitinib group after both the first dose ($P = 0.048$) and the last dose ($P = 0.001$), indicating reduced systemic exposure to artemether (table S6). Artemether is quickly hydrolyzed to its active metabolite, DHA. The mean C_{max} for DHA was 59.93 ng/ml (SD 1.62) in the placebo group compared with 41.45 ng/ml (SD 1.28) in the ruxolitinib group after the first dose

Table 2. Overall summary of AE incidence and severity after ruxolitinib or placebo dosing in the first inoculation phase (day 8 to day 89). *n* (%), number and percentage of participants experiencing an AE; *E*, number of AEs; IMP, investigational medicinal product (ruxolitinib/placebo); SAE, serious adverse event.

	Ruxolitinib (*N* = 11)		Placebo (*N* = 9)		Total (*N* = 20)	
	n (%)	*E*	*n* (%)	*E*	*n* (%)	*E*
Any AE	9 (81.8%)	51	9 (100.0%)	73	18 (90.0%)	124
Mild	8 (72.7%)	35	9 (100.0%)	51	17 (85.0%)	86
Moderate	7 (63.6%)	15	5 (55.6%)	19	12 (60.0%)	34
Severe	1 (9.1%)	1	2 (22.2%)	3	3 (15.0%)	4
IMP-related AE	8 (72.7%)	17	5 (55.6%)	18	13 (65.0%)	35
Mild	5 (45.5%)	7	4 (44.4%)	9	9 (45.0%)	16
Moderate	5 (45.5%)	9	3 (33.3%)	7	8 (40.0%)	16
Severe	1 (9.1%)	1	1 (11.1%)	2	2 (10.0%)	3
Challenge agent–related AE	8 (72.7%)	37	6 (66.7%)	47	14 (70.0%)	84
Mild	7 (63.6%)	23	6 (66.7%)	32	13 (65.0%)	55
Moderate	6 (54.5%)	13	5 (55.6%)	12	11 (55.0%)	25
Severe	1 (9.1%)	1	2 (22.2%)	3	3 (15.0%)	4
SAE	0 (0.0%)	0	0 (0.0%)	0	0 (0.0%)	0

Table 3. Ruxolitinib- and placebo-related AEs. *n* (%), number and percentage of participants experiencing an AE; *E*, number of AEs.

AE preferred term	Ruxolitinib (*N* = 11)		Placebo (*N* = 9)		Total (*N* = 20)	
	n (%)	*E*	*n* (%)	*E*	*n* (%)	*E*
Abdominal discomfort	1 (9.1%)	1	1 (11.1%)	1	2 (10.0%)	2
ALT increased	1 (9.1%)	1	1 (11.1%)	1	2 (10.0%)	2
Aspartate aminotransferase increased	0 (0.0%)	0	1 (11.1%)	1	1 (5.0%)	1
γ-Glutamyltransferase increased	0 (0.0%)	0	1 (11.1%)	1	1 (5.0%)	1
Hemoglobin decreased	3 (27.3%)	3	1 (11.1%)	1	4 (20.0%)	4
Headache	3 (27.3%)	3	3 (33.3%)	4	6 (30.0%)	7
Hyperhidrosis	0 (0.0%)	0	1 (11.1%)	2	1 (5.0%)	2
Lymphocyte count decreased	2 (18.2%)	2	2 (22.2%)	2	5 (25.0%)	5
Nausea	1 (9.1%)	1	2 (22.2%)	3	3 (15.0%)	4
Neutrophil count decreased	2 (18.2%)	4	0 (0.0%)	0	2 (10.0%)	4
Platelet count decreased	1 (9.1%)	1	0 (0.0%)	0	1 (5.0%)	1
White blood cell count decreased	1 (9.1%)	1	2 (22.2%)	2	3 (15.0%)	3

($P = 0.095$). The C_{max} was significantly different after the last dose, with values of 71.05 ng/ml (SD 2.30) and 27.89 ng/ml (SD 2.17) for placebo and ruxolitinib groups, respectively ($P = 0.019$; table S6 and fig. S1C). The AUC for DHA was significantly lower in ruxolitinib-treated individuals ($P = 0.005$). In contrast with artemether and DHA, ruxolitinib had no impact on concentrations of lumefantrine or DBL (table S7 and fig. S1, D and E).

Parasite clearance after first inoculation and treatment with artemether-lumefantrine plus ruxolitinib or placebo

Parasite clearance was evaluated using the parasite reduction ratio over 48 hours (PRR_{48}) and the parasite clearance half-life ($PC_{t1/2}$), estimated using the slope of the optimal fit of the log-linear relationship of the parasite decay (*18*). All participants in the ruxolitinib group had significant ($P < 0.001$) regression models (slope

coefficient from the log-linear parasite decay regression) and contributed toward the treatment-specific estimate of PRR_{48} and corresponding $PC_{t1/2}$. However, in the placebo group, only seven of nine participants had significant ($P < 0.001$) regression models and contributed toward the parasite clearance parameter estimates (table S8). The PRR_{48} was significantly lower in the ruxolitinib group {2827 [95% confidence interval (CI) 2344 to 3409]} compared with the placebo group [8242 (95% CI 6117 to 11104)] ($Q_B = 35.5$, $P < 0.001$) (table S9). However, this difference was no longer significant in a sensitivity analysis that removed one outlying participant in the placebo group who had particularly rapid parasite clearance (R007) ($Q_B = 0.56$, $P = 0.45$; table S9). No participant experienced recrudescence.

Ruxolitinib reduces IL-6–induced STAT phosphorylation in myeloid and $CD4^+$ T cells

To assess the impact of ruxolitinib on cell signaling, STAT1, STAT3, and STAT5 phosphorylation was measured after IL-6 stimulation of whole blood. Samples were collected immediately before inoculation (baseline), immediately before treatment, 1 day after treatment (2 hours after ruxolitinib/placebo dose 3), and 5 days after treatment. Whole blood was stimulated with the JAK/STAT-activating cytokine IL-6 or left unstimulated for 15 min, and STAT phosphorylation (pSTAT) was assessed in myeloid cells and $CD4^+$ T cells using phosphor-cytometry by time-of-flight (pCyTOF) (Fig. 2A and table S10). After batch correction, myeloid cells and $CD4^+$ T cells were identified on the basis of expression of cell lineage markers (Fig. 2B).

IL-6 stimulation increased phosphorylation of STAT1, STAT3, and STAT5 in both myeloid and $CD4^+$ T cells (Fig. 2C). IL-6–induced expression of pSTAT1 and pSTAT3 on myeloid cells was significantly increased ($P < 0.001$) on the day of treatment compared with baseline (Fig. 2D), indicating that infection with *P. falciparum* increased sensitivity of myeloid cells to IL-6. There was no increase in expression of pSTAT1 or pSTAT3 on $CD4^+$ T cells before treatment, and IL-6–induced pSTAT5 expression decreased on myeloid and $CD4^+$ T cells (Fig. 2, D and E). After treatment, there was a decrease in IL-6–induced expression of pSTAT1 and pSTAT3 in myeloid and $CD4^+$ T cells in the ruxolitinib group, whereas pSTAT1 expression increased in the placebo group (Fig. 2, D and E). pSTAT5 was decreased by ruxolitinib treatment in $CD4^+$ T cells but not myeloid cells. The fold change reductions in IL-6–induced pSTAT1 and pSTAT3 expression on myeloid cells and pSTAT1 expression on $CD4^+$ T cells were correlated with ruxolitinib AUC (Fig. 2, F and G).

Ruxolitinib attenuated posttreatment changes in hematological and biochemical parameters

As previously observed in malaria volunteer infection studies (*19*–*21*), reductions in hemoglobin, platelets, and lymphocytes occurred in both treatment groups after inoculation (Fig. 3, A to C). Hemoglobin reached a nadir 7 days after treatment, with no difference between treatment groups. In the placebo group, platelets and lymphocytes also decreased after treatment, reaching nadirs on days 3 and 1, respectively. These posttreatment reductions were not observed in the ruxolitinib group, with a significant impact of ruxolitinib observed on day 3 for platelets ($P = 0.022$) and day 1 for lymphocytes ($P < 0.001$). Neutrophils declined after treatment in both groups, reaching a nadir on day 3, with no difference observed between treatment groups (Fig. 3D).

The inflammatory marker C-reactive protein [CRP; measured by enzyme-linked immunosorbent assay (ELISA)] increased in both groups after inoculation. After treatment, CRP increased further in the placebo group but not in the ruxolitinib group, with a significant ($P < 0.001$) impact of ruxolitinib treatment on days 1 to 3 posttreatment (Fig. 3E). The peak CRP posttreatment correlated with the pretreatment parasitemia in the placebo group ($r = 0.80$, $P = 0.013$) but not in the ruxolitinib group ($r = -0.04$, $P = 0.91$). The peak CRP was also associated with the total malaria clinical score during the confinement period ($r = 0.64$, $P = 0.003$) (table S3). As previously observed in malaria volunteer infection studies (*22*, *23*), ALT increased modestly after treatment; this increase was delayed in the ruxolitinib group, with an impact of treatment observed on days 1 to 3 posttreatment (Fig. 3F).

Ruxolitinib attenuated the posttreatment inflammatory response to the initial infection

The impact of ruxolitinib on antiparasitic immune responses was assessed by quantifying IFN-γ and IL-10 within culture supernatants after restimulation of peripheral blood mononuclear cells (PBMCs) with parasite-infected RBCs or uninfected RBCs (uRBCs) for 72 hours (*9*). In both treatment groups, IFN-γ and IL-10 production increased by day 7 posttreatment, and IL-10 production was higher in the ruxolitinib group compared with the placebo group at this time point (fig. S2A). However, mixed model analysis did not demonstrate an effect of ruxolitinib on the increase of IFN-γ and IL-10 at day 7 posttreatment (interaction term $P > 0.05$; fig. S2B). Further, the mixed model analysis suggested that at the day 3 time point, ruxolitinib attenuated the posttreatment increase in IL-10 (fig. S2B). The impact of ruxolitinib was further assessed on other cytokines in poststimulation supernatants quantified in Luminex ($n = 46$), using the mixed model analysis. At day 7 posttreatment, other inflammatory markers, including macrophage inhibitory protein-1α (MIP-1α), MIP-1β, and tumor necrosis factor–α (TNF-α), were increased in both treatment groups; however, this increase did not appear to be affected by ruxolitinib (fig. S2, C and D, and data file S4).

The impact of ruxolitinib on the host response after treatment was further assessed by Alamar nucleic acid linked immuno-sandwich assay (NULISA) on plasma collected before inoculation; before treatment; and days 3, 7, and 21 posttreatment. Inflammatory markers known to be associated with disease severity in malaria, including IL-6 (*24*), the endothelial activation marker angiopoietin-2 (*25*), intercellular adhesion molecule-1 (ICAM-1) (*26*), and syndecan-1 (a marker of breakdown of endothelial glycocalyx) (*27*), were analyzed. Of these, IL-6 and ICAM-1 increased significantly ($P < 0.001$) from preinoculation to day of treatment, whereas angiopoietin-2 decreased (Fig. 4, A to D). After treatment, angiopoietin-2, ICAM-1, and syndecan-1 all increased in the placebo group, with ICAM-1 peaking at day 3 and angiopoietin-2 and syndecan-1 peaking at day 7 (Fig. 4, A to D). These posttreatment increases were either not observed, or reduced, in the ruxolitinib group, with a significant impact ($P < 0.05$) of treatment on day 3 posttreatment for ICAM-1; days 3, 7, and 21 for angiopoietin-2; and day 7 for syndecan-1.

To further examine the impact of ruxolitinib on the host response, the entire panel of analytes was assessed ($n = 250$). *P. falciparum* infection induced a host response in both groups, with 139 (55.6%) analytes increased and 7 (2.8%) decreased between

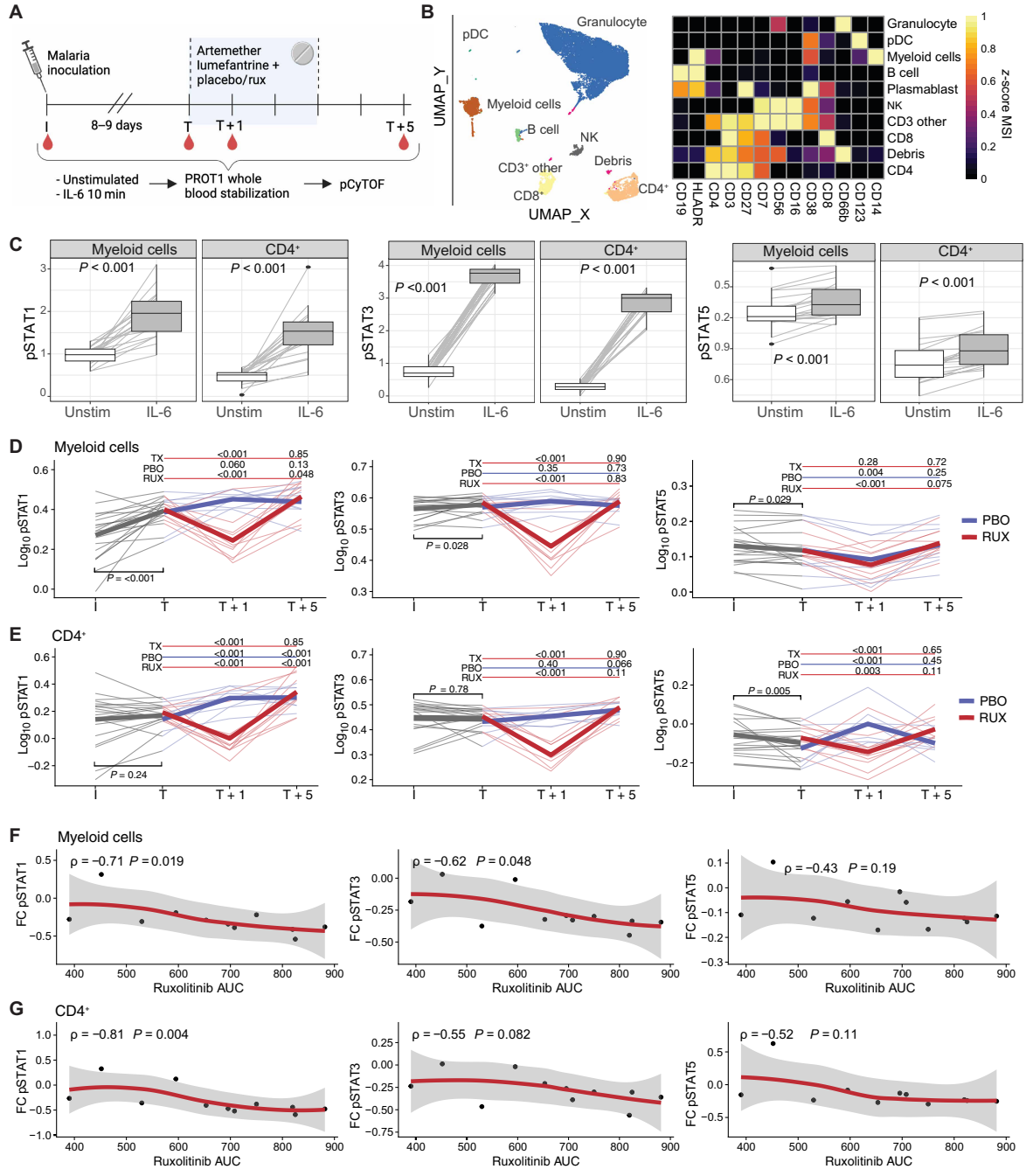

Fig. 2. Ruxolitinib treatment affected signaling in myeloid cells and CD4$^+$ T cells. (**A**) Whole blood was collected at inoculation (I), treatment (T), T + 1 (2 hours after third dose of ruxolitinib or placebo), and T + 5 days, for $n = 20$ participants at each time point. Blood was stimulated with IL-6 or left unstimulated, fixed in PROT1, and analyzed by pCyTOF. (**B**) Cell subsets were identified by expression profiles of linage markers and are presented in a uniform manifold approximation and projection (UMAP) plot (left) and heatmap (right). NK, natural killer; PDC, plasmacytoid dendritic cell. (**C**) pSTAT1, pSTAT3, and pSTAT5 expression as median signaling intensity (MSI) values in myeloid cells and CD4$^+$ T cells in unstimulated and IL-6–stimulated samples at inoculation. Data are Tukey box plots with the median and 25th and 75th percentiles. The top and bottom hinges extend to the largest and smallest values, respectively, but no further than 1.5× IQR from the hinge. *P* values were calculated by Wilcoxon signed-rank test. (**D** and **E**) pSTAT1, pSTAT3, and pSTAT5 expression in myeloid cells (D) and CD4$^+$ T cells (E) at I, T, T + 1, and T + 5. Data are log-transformed median signaling intensity, with thin lines representing individuals and colored by treatment group. Before randomization is in gray, after randomization ruxolitinib individuals are red, and placebo are blue. *P* values are from linear mixed-effect models, with bold lines representing the mean of the predicted values from the fitted models for each group. TX represents the FDR-corrected *P* values for the interaction term between each time point (relative to time point T) and treatment group, i.e., the difference in change from the baseline between the ruxolitinib and placebo groups. FDR-corrected *P* values for the comparison between each time point and time point T are shown for the placebo (PBO) and ruxolitinib (RUX) groups and were determined from contrasts. (**F** and **G**) Fold change (FC) of MSI of pSTAT1/3/5 at time point T compared with time point T + 1 in the ruxolitinib-treated group in myeloid (F) or CD4$^+$ T cells (G), correlated with ruxolitinib area under the curve (AUC). The red lines are locally estimated scatterplot smoothing (LOESS) fit curves with error bands of 95% CI in gray shaded regions. Spearman's rho and *P* are indicated.

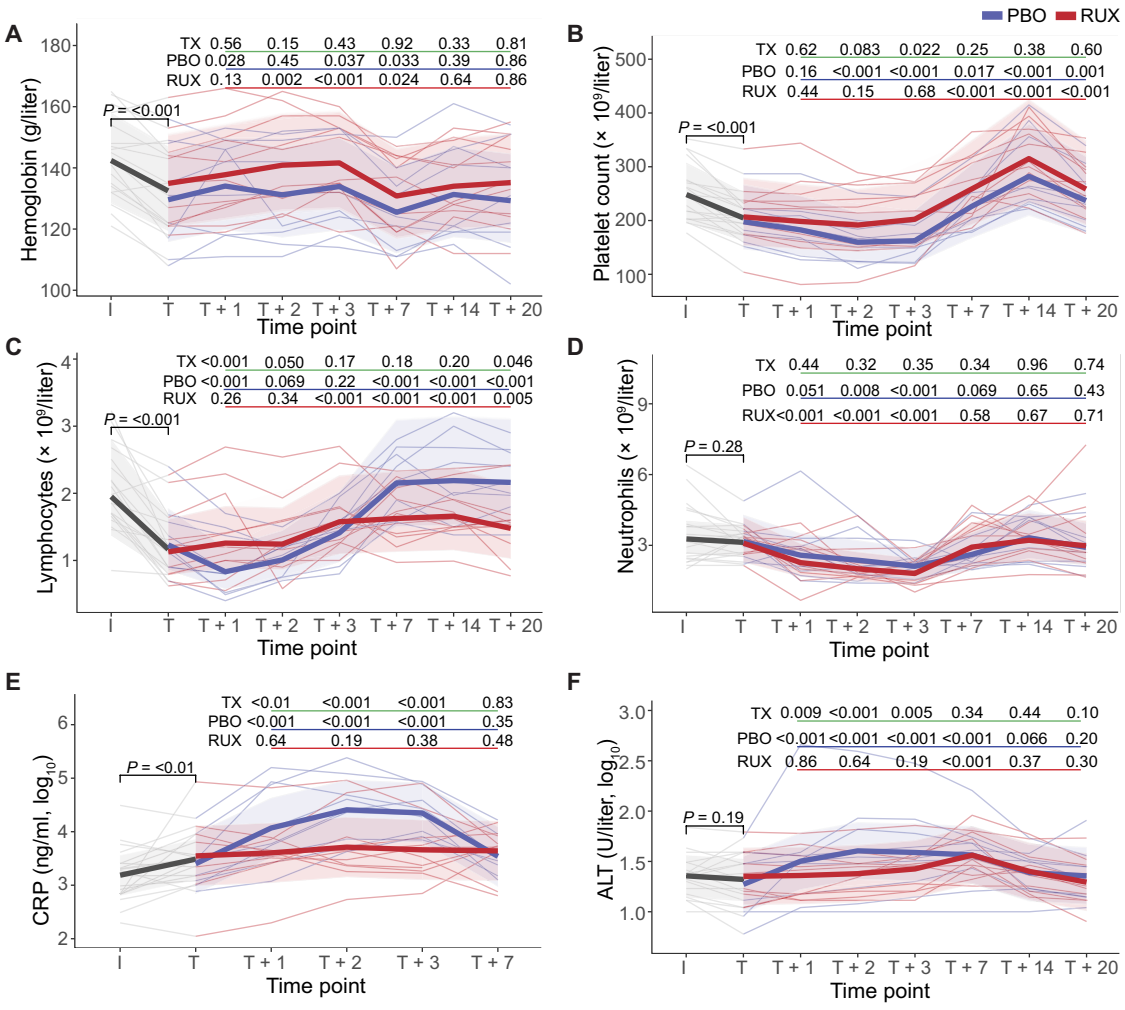

Fig. 3. Ruxolitinib lessened infection-induced changes to hematological and biochemical parameters. (**A** to **F**) Hematological and biochemical parameters including hemoglobin concentration (A), platelet count (B), lymphocyte count (C), neutrophil count (D), CRP concentration (E), and ALT concentration (F) at inoculation (I), treatment (T), and 3, 7, and 21 days after treatment (T + 3, T + 7, and T + 21). Data are raw data (log-transformed for CRP and ALT) with thin lines representing individuals and colored by treatment group (blue for placebo, red for ruxolitinib treatment groups), and bold lines representing the mean of the predicted values from the fitted models for each group. *P* values are FDR-corrected from linear mixed-effect models. TX represents the FDR-corrected *P* values for the interaction term between each time point (relative to time point T) and treatment group, i.e., the difference in change from baseline between the ruxolitinib and placebo groups (underlined in green). FDR-corrected *P* values for the comparison between each time point and time point T are shown for the placebo (PBO, underlined with blue) and ruxolitinib (RUX, underlined with red) groups and were determined from contrasts.

inoculation and treatment [false discovery rate (FDR)–corrected; fig. S3, A and B, and data file S5]. IFN-γ was the most up-regulated analyte, with other inflammatory markers, including TNF-α, chemokine (C-X-C motif) ligands (CXCL) 9/10/11, chemokine (C-C motif) ligand (CCL) 4, IL-6, and CRP, also up-regulated (fig. S3, A and B). Pathway analysis of up-regulated analytes identified an inflammatory response, with TNF signaling via nuclear factor kappa-light-chain-enhancer of activated B cells and IL-2/STAT4 signaling and IL-6/JAK/STAT3 signaling among the top up-regulated pathways (fig. S3C).

After treatment, in the placebo group, there were 115 analytes that had changed at day 3 posttreatment (compared with the treatment time point), including 96 of 250 (38.4%) that increased and 19 of 250 (7.6%) that decreased (Fig. 4E). Of these 115 analytes, an impact of ruxolitinib was detected for 30 (26.1%) analytes, 24 (20.1%) of which were down-regulated and 6 (5.2%) of which were increased (Fig. 4F). Analytes down-regulated by ruxolitinib included CRP (confirming the above analysis where CRP was quantified by ELISA) and TNF receptor superfamily member 14 (also known as LIGHT), blockade of which we have previously shown protects against experimental cerebral malaria (Fig. 4G) (*28*). The effect of ruxolitinib on angiopoietin-2 at days 3 and 7 posttreatment remained significant after FDR correction for all analytes ($P = 0.004$ and $P = 0.04$, respectively). Pathway analysis identified that ruxolitinib was associated with down-regulation of IL-6/JAK/STAT3 signaling and an attenuated inflammatory response (fig. S3D). Exploratory correlation analysis between NULISA analytes from ex vivo plasma and Luminex analytes from in vitro parasite stimulated cultures identified few correlations between the data modules at all time points, indicating distinct immune responses quantified with each approach (fig. S3E).

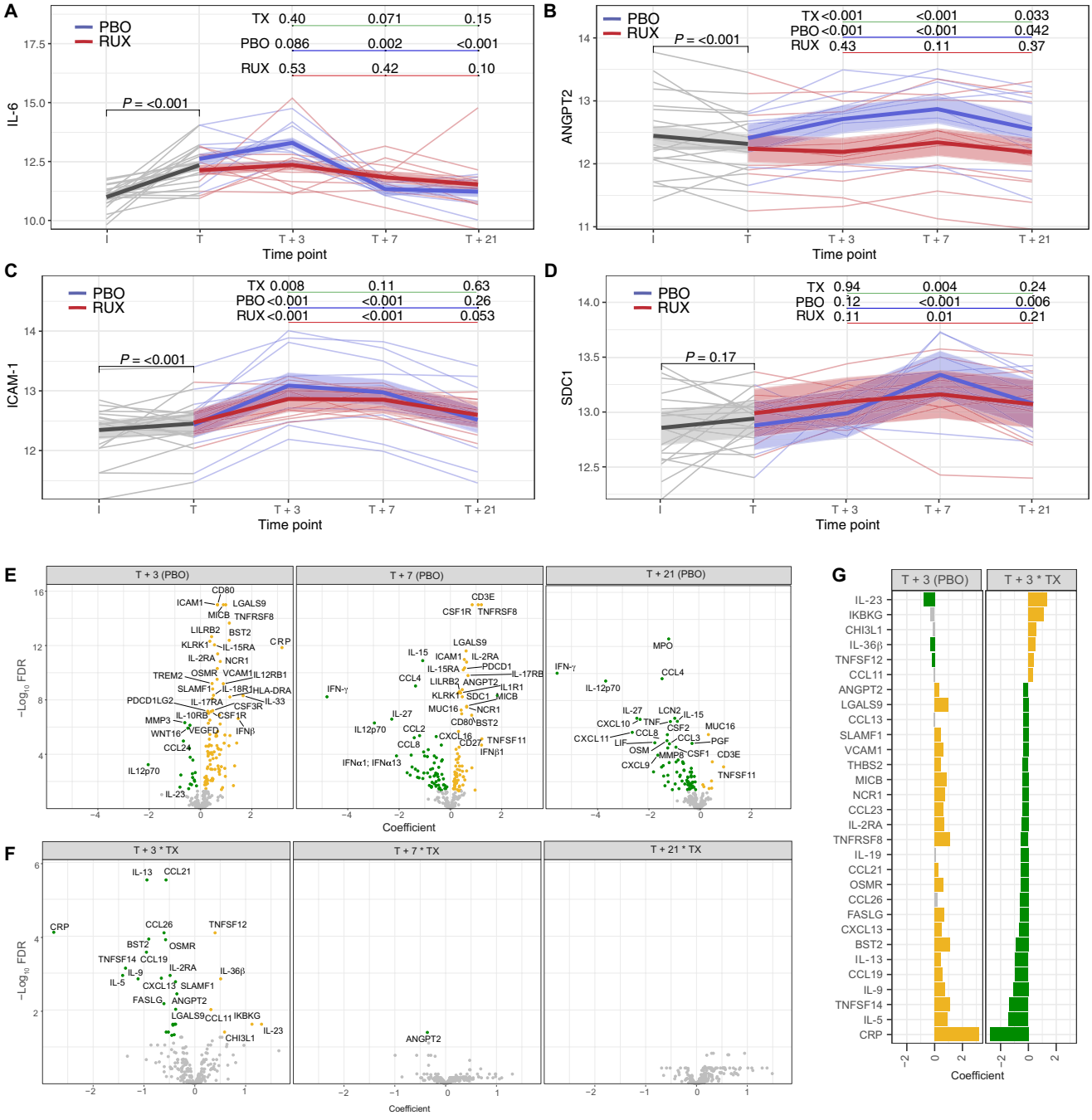

Fig. 4. Ruxolitinib alleviated systemic inflammatory responses. Alamar NULISA was used to quantify 250 analytes in plasma at inoculation (I), treatment (T), and 3, 7, and 21 days after treatment (T + 3, T + 7, and T + 21). (**A** to **D**) Shown are concentrations of IL-6 (A), angiopoietin-2 (ANGPT2) (B), ICAM-1 (C), and syndecan-1 (SDC1) (D) over the course of trial. Data are log-transformed with thin lines representing individuals and colored by treatment group (gray before inoculation, red in ruxolitinib-treated, and blue in placebo groups) and bold lines representing the mean of the predicted values from the fitted models for each group. *P* values (unadjusted) are from linear mixed-effect models. TX represents the *P* values (unadjusted) for the interaction term between each time point (compared with time point T) and treatment group, i.e., the difference in change from baseline between the ruxolitinib and placebo groups (underlined in green). *P* values (unadjusted) for the comparison between each time point and time point T are shown for the placebo (PBO, underlined with blue) or ruxolitinib (RUX, underlined with red) group and were determined from contrasts. (**E**) Volcano plots show coefficient estimates from linear mixed-effects models and $-\log_{10}$(FDR) of changes of analyte at each time point compared with T in the placebo group. Coefficient estimates from linear mixed-effects models and FDR values are from linear mixed-effect model analysis. Analytes that are up-regulated relative to time point T are in gold and down-regulated in green. (**F**) Volcano plots show coefficient estimates and $-\log_{10}$(FDR) of interaction terms between the ruxolitinib treatment group and change of analyte at each time point compared with time point T. Coefficient and FDR values are from linear mixed-effect model analysis. Analytes that are up-regulated compared with the change in placebo are in gold, and those that are down-regulated compared with the change in placebo are in green. (**G**) Shown are individual analytes at T + 3 that were modified by ruxolitinib. Data are the coefficient estimates from linear mixed-effects models for the change compared with time point T in the placebo group [T + 3 (PBO)] and the coefficient estimates from linear mixed-effects models for the interaction term between time and ruxolitinib treatment (T + 3 * TX).

Ruxolitinib enhanced the immune memory response after second inoculation

To assess the impact of ruxolitinib on antiparasitic immune responses to reinfection, participants were reinoculated with the same *P. falciparum* 3D7 strain 90 days after the first infection. After the second infection, there was no difference in time to parasitemia between treatment groups (table S11; Fisher's exact, $P = 0.29$). However, in both groups, the parasite multiplication rate over 48 hours (PMR_{48}) and overall parasite growth rate were reduced (tables S12 and S13), with a sensitivity analysis showing that the parasite growth rate was 0.08 $\log_{10}$ parasites/ml per day lower (95% CI 0.02 to 0.14) in the second infection compared with the first ($P = 0.009$) (table S14). There was no evidence that this reduced parasite growth rate differed between treatment groups [log-likelihood ratio test, $\chi^2(2) = 4.24$, $P = 0.12$; table S14].

To evaluate memory immune responses to the second infection, NULISA data were analyzed using segmented regression to identify analytes that changed between the first and second infections and to determine whether these differences were modulated by ruxolitinib. Analyte responses were compared at matched time points across both infections; for individuals treated later during the second infection, day 7 postinoculation was used to avoid confounding from prolonged parasite exposure.

Consistent with a memory response and improved parasite control during the second infection, 82 analytes (of 248, 33.1%) showed differential responses compared with the first infection, with 38 (15.3%) up-regulated and 44 (17.7%) down-regulated (Fig. 5A). Up-regulated analytes included markers of inflammation, such as CRP, CXCL9, CXCL10, granzyme A (GZMA), granzyme B (GZMB), and IFN-α1/IFN-α13 (Fig. 5B). Immunoregulatory molecules including interleukin-18 binding protein (IL-18BP; FDR = 0.003) and lymphocyte-activation gene 3 (LAG3; FDR = 0.009) were also increased (Fig. 5A). In addition, for 26 analytes (10.5%), the change in response in the second infection was modified by ruxolitinib (Fig. 5C). This included increased 4-1BB (TNFRSF9/CD137) and human leukocyte antigen–DR isotype alpha chain (HLA-DR) concentrations, consistent with increased T cell activation (Fig. 5D), and increased chitinase-3–like protein 1 (CHI3L1) and leukemia inhibitory factor (LIF) concentrations, associated with tissue repair and homeostasis (Fig. 5D) (interaction phase*treatment 4-1BB FDR = 0.006, HLA-DR FDR = 0.031, CHI3L1 FDR < 0.001, LIF FDR = 0.006) (*29*, *30*). Together, these data support the generation of a memory immune response after reinfection with *P. falciparum*, which was further enhanced by ruxolitinib.

DISCUSSION

In this randomized, placebo-controlled trial in malaria-naive volunteers infected with *P. falciparum*, adjunctive therapy with ruxolitinib was safe and well tolerated, transiently suppressed cellular pSTAT signaling, and attenuated the inflammatory response after antimalarial treatment. In addition, analysis of plasma biomarkers after a second infection revealed an induced memory immune response, which was enhanced in ruxolitinib-treated participants. These findings highlight the potential of ruxolitinib as an adjunctive therapy to improve clinical outcomes and promote the development of antiparasitic immunity in malaria.

This study was based on the hypothesis that ruxolitinib, a JAK 1/2 inhibitor, would block type-1 IFN signaling and thereby modulate the immunoregulatory networks that hinder the development of antiparasitic immunity after natural malaria infection or vaccination (*6*). We first confirmed that ruxolitinib inhibited JAK/STAT signaling by demonstrating that ruxolitinib reduced IL-6–induced phosphorylation of STAT1 and STAT3 in myeloid and $CD4^+$ T cells and STAT5 in $CD4^+$ T cells. These data are supported by subsequent analyses that showed that ruxolitinib reduced IFN-β–induced phosphorylation of these pathways (*31*). These inhibitory effects correlated with plasma ruxolitinib concentration, providing further evidence of effective suppression of JAK/STAT signaling and supporting the role of ruxolitinib in inhibiting type I IFN activity.

A key finding in this study was the impact of ruxolitinib on the posttreatment inflammatory response, evaluated with standard hematological and biochemical parameters, as well as with the sensitive NULISA platform. As expected, biomarkers of inflammation were increased in participants after inoculation with *P. falciparum* (*9*, *20*). In the placebo group, this response increased further after antimalarial treatment, with the key inflammatory marker CRP peaking 2 to 3 days after treatment. Other key markers of disease severity also increased after treatment, including angiopoietin-2 and ICAM-1, markers of endothelial activation (*32*) and cytoadherence (*33*), respectively, and both are associated with disease severity in falciparum malaria (*25*, *26*, *34*, *35*). The posttreatment increase in these inflammatory markers likely reflects the host response to the release of parasite antigens after rupture of infected RBCs and may contribute to the high mortality from severe malaria even after commencing antiparasitic treatment (*2*). Although this inflammatory response is a key target for adjunctive therapies in severe malaria, no adjunctive treatment has yet been shown to reduce mortality (*36*). Here, we found that ruxolitinib substantially attenuated posttreatment increases in CRP, angiopoietin-2, and ICAM-1. Moreover, peak CRP concentration in placebo-treated participants correlated strongly with pretreatment parasitemia, whereas this correlation was absent in the ruxolitinib group, further supporting the role of ruxolitinib in inhibiting the parasite-induced inflammatory process. These data are consistent with the anti-inflammatory effects of ruxolitinib in in vitro models (*37*) and in a preclinical severe malaria model (*38*) and the reductions in inflammatory biomarkers observed when ruxolitinib is used in myeloproliferative disorders (*39*). Further, a recent study involving a three-dimensional blood-brain barrier model demonstrated that ruxolitinib prevented JAK/STAT-mediated increases in blood-brain barrier permeability after exposure to parasite egress products (*40*). Together, these data suggest a potential role for adjunctive ruxolitinib for improving outcomes in severe malaria.

Our data provide support for the safety of ruxolitinib in malaria. Participants who received ruxolitinib did not experience more AEs. Moreover, ruxolitinib was associated with reduced concentrations of artemether and its active metabolite, DHA, and with slower parasite clearance. Although the latter appeared largely driven by one placebo-treated participant with particularly rapid parasite clearance, parasite clearance dynamics should be closely monitored in future trials of adjunctive ruxolitinib therapy.

The impact of ruxolitinib on the development of long-lasting antiparasitic immunity in this study was evaluated by subjecting participants to a second *P. falciparum* infection 3 months after the first. After reinfection, both treatment groups exhibited elevated concentrations of immune biomarkers associated with parasite control. These included chemokines like CCL19, which facilitates $CD4^+$ T

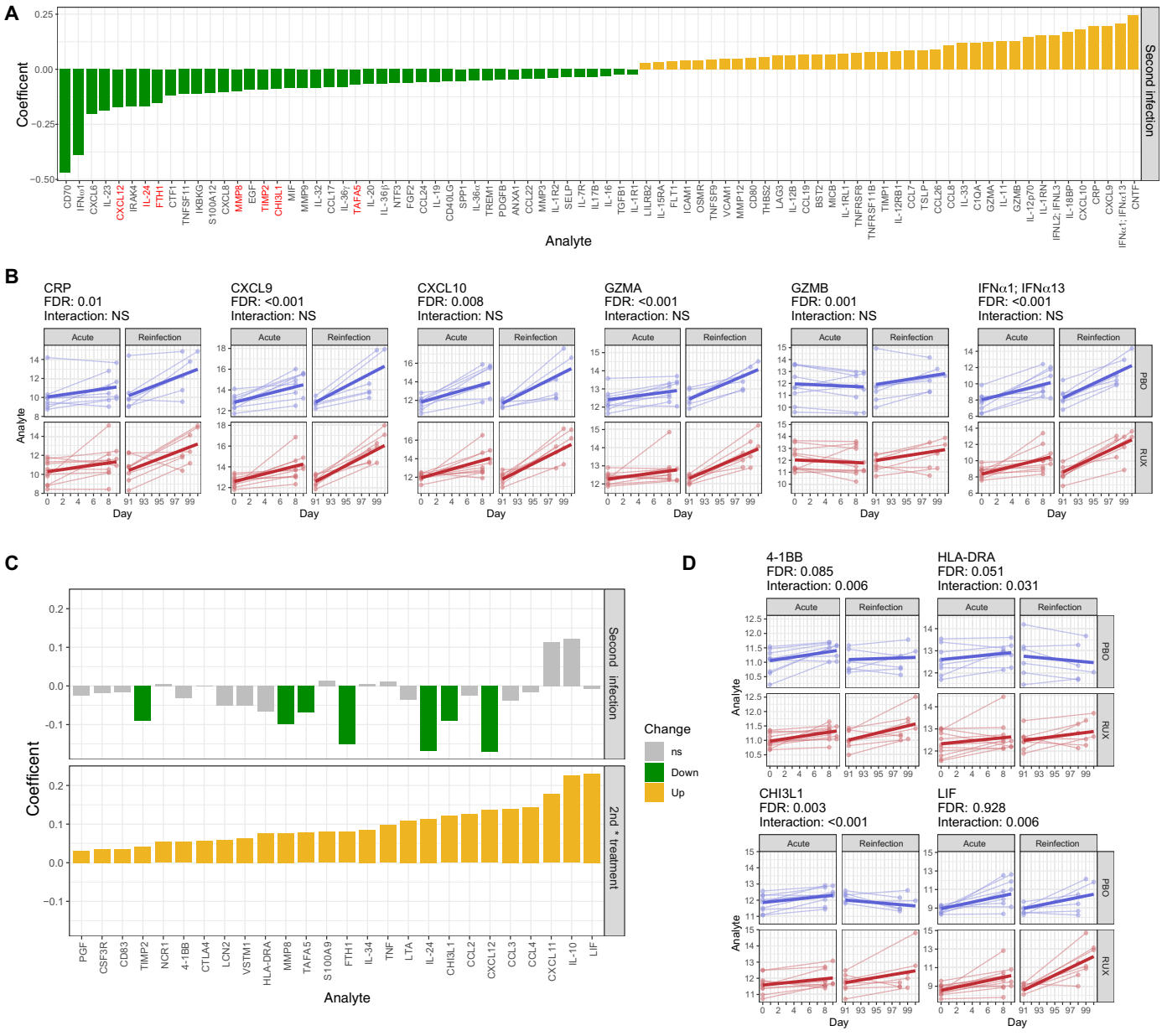

Fig. 5. Ruxolitinib was associated with an improved immune response to second *P. falciparum* infection. (**A**) Coefficient for the change in slope between first and second infections for each analyte with an FDR for a difference of <0.05. The change in response of analytes in red was modified by ruxolitinib. (**B**) Concentration of analytes CRP, CXCL9, CXCL11, GZMA, GZMB, and IFN-α1/IFN-α13 between inoculation and treatment in first and second infection in placebo (PBO)– and ruxolitinib-treated (RUX) groups. FDR indicates a significant difference in the slopes for each analyte between infections. Interaction [all nonsignificant (NS)] indicates the interaction term for an impact of treatment on the change in induction between infections. (**C**) Coefficient for the change in slope between first and second infections and for the interaction term of impact of treatment group for all analytes where the interaction term FDR was <0.05. Change for second infection is on the top, and impact of treatment is on the bottom (second * treatment). Nonsignificant (NS) changes in the second infection only are in gray. (**D**) 4-1BB, HLA-DR, CHI3L1, and LIF responses in the first and second infections in placebo- and ruxolitinib-treated individuals. FDR indicates a significant difference in slope between the first and second infections, and interaction indicates the FDR value for the impact of ruxolitinib on the change in slope.

cell trafficking to secondary lymphoid tissues (*41*); inflammatory markers including CRP, GZMB, and GZMA; and immunoregulatory molecules like IL-19BP and LAG3. Ruxolitinib treatment during the first infection may have improved the quality of memory and recall immune responses. Specifically, ruxolitinib treatment was associated with increased expression of T cell activation markers such as HLA-DR and 4-1BB, as well as tissue repair factors including LIF (*30*) and CHI3L1 (*29*). These findings suggest that ruxolitinib treatment during primary infection may have enabled a durable immunological imprint that modulated the response to subsequent infection. Although such imprinting is well established in viral infections (*42*), its relevance in malaria is only beginning to be appreciated (*6*). Analysis of $CD4^+$ T cell responses induced during this study indicates that ruxolitinib treatment modulated $CD4^+$ T cell development

(*31*). Further work is needed to define the specific immune cell populations targeted by ruxolitinib and to clarify its broader effects on host immunity, including the magnitude and quality of humoral responses.

The link between ruxolitinib-induced changes in memory responses and parasite control remains unresolved. Although participants receiving ruxolitinib showed evidence of enhanced immune memory, this did not translate into reduced parasite growth during secondary infection, as measured by PMR_{48}. Although the study was underpowered to detect significant differences in PMR_{48}, the findings suggest that enhanced memory responses may be distinct from the mechanisms required for acute parasite control or that they represent an early stage of immunity not yet sufficient to influence parasite clearance.

An important consideration for the interpretation of our findings is that this study was conducted in malaria-naïve volunteers in Australia, with treatment administered very early in the course of infection. The impact of ruxolitinib on the posttreatment inflammatory response may differ in individuals with clinical malaria and higher parasitemia. Further, in malaria-endemic regions, individuals may have preexisting immunity from prior infections, and the effects of adjunctive ruxolitinib on the development of immune responses may differ from those observed in the current study. Studies in malaria-exposed populations will be critical to test the potential of adjunctive ruxolitinib for both improving clinical outcomes and the development of antiparasitic immunity.

Several other limitations were apparent in this study. First, because of recruitment challenges and the COVID-19 pandemic, only 20 of the planned 26 participants were enrolled, and only 15 proceeded to a second infection. This reduced our statistical power to detect between-group differences, such as in parasite growth after reinfection. Nonetheless, we observed significant differences in inflammatory and immune responses between treatment groups. Second, in the analysis of parasite clearance, two participants in the placebo group had nonsignificant regression models and were excluded, and one participant appeared to be an outlier with particularly rapid parasite clearance. Thus, uncertainty exists around the impact of ruxolitinib on parasite clearance. Third, plasma samples for NULISA analysis were only collected on days 3, 7, and 21 after treatment of the first infection, and impacts of adjunctive ruxolitinib within 24 to 48 hours of treatment may have been missed. Last, PBMC stimulation with parasite antigens was only performed with a single PBMC:*P. falciparum*–infected RBC (pRBC) ratio, potentially masking some antigen-specific immune responses.

In conclusion, this randomized placebo-controlled trial in volunteers infected with *P. falciparum* demonstrated that adjunctive ruxolitinib was safe and well tolerated and reduced the posttreatment inflammatory response while enhancing immune memory responses to reinfection. Although the potential impact of ruxolitinib on parasite clearance warrants further investigation, these findings provide support for advancing ruxolitinib as an adjunctive therapy to improve clinical outcomes and enhance antiparasitic immunity after natural infection or vaccination.

MATERIALS AND METHODS

Study design

This was a randomized, double-blind, placebo-controlled, phase 1b clinical trial using the *P. falciparum*–induced blood stage malaria (IBSM) model to assess whether ruxolitinib can modulate host immune responses and enhance protective immunity when administered with artemether-lumefantrine. Healthy malaria-naïve males and females (nonpregnant, nonlactating) aged 18 to 55 years were eligible for inclusion (full eligibility criteria are in the Clinical Trial Protocol; data file S6). The study was conducted at the University of the Sunshine Coast Clinical Trails Unit (Morayfield, Australia) and was registered on the Australian New Zealand Clinical Trials Registry on 6 July 2021 (ACTRN12621000866808, https://anzctr.org.au/Trial/Registration/TrialReview.aspx?ACTRN=12621000866808). This study was approved by the QIMR Berghofer Human Research Ethics Committee (P3696) and ethically reviewed in minimizing duplication of ethics by the Australian Departments of Defence and Veterans' Affairs Human Research Ethics Committee. All participants gave written informed consent. The primary outcome was the incidence, severity, and causality of AEs. Secondary outcomes were parasite growth parameters (time to parasitemia and PMR_{48}), parasite clearance kinetics (PRR_{48} and $PC_{t1/2}$), drug pharmacokinetic (PK) parameters, immune and inflammatory response parameters, and pSTAT3 inhibition.

The planned sample size was 26 participants, randomized 1:1 to ruxolitinib and placebo. This was based on the secondary outcome of the antiparasitic immune response (IFN-γ and IL-10 concentration). Sample size calculations used data from a study that measured cytokine production after *P. falciparum* parasite stimulation of PBMCs collected from participants in previous *P. falciparum* IBSM trials (*9*). With 13 participants per group in the current study, a two-sided two sample *t* test was estimated to have 80% power to detect a 23% difference in mean IFN-γ concentration 7 days posttreatment and 8% difference in mean IL-10 concentration at the same time point, with a type I error rate of 5%. This sample size was also considered appropriate to assess the primary outcome associated with safety and tolerability.

The randomization list was generated electronically by an unblinded statistician using STATA 15. A copy of the randomization schedule was sent to the unblinded clinical unit pharmacist and one other staff member. All remaining investigators, participants, clinical staff, and the study statistician remained blinded until unblinding was performed at the time of database lock. Dosing was performed by the unblinded staff member, and participants were blindfolded because ruxolitinib and placebo tablets were not matched in terms of appearance.

Procedures

Participants were inoculated intravenously with ~2800 viable *P. falciparum* 3D7–infected human erythrocytes on day 0. On day 9 (cohorts 1 and 2) or day 8 (cohorts 3 to 6), participants were admitted to the clinical unit and randomized in a 1:1 ratio to receive oral twice daily doses of artemether-lumefantrine (Riamet, Novartis Pharmaceuticals) in conjunction with either ruxolitinib (Jakavi, Novartis Pharmaceuticals) or placebo (microcrystalline cellulose, PCI Pharma). Artemether-lumefantrine dosing was in accordance with the manufacturer recommendations for treatment of malaria [four tablets (each containing 20 mg of artemether and 120 mg of lumefantrine) twice daily over 3 consecutive days with food or drink rich in fat]. One ruxolitinib tablet (20 mg) or one placebo tablet was administered with 250 ml of water 2 hours after each artemether-lumefantrine dose (total course of six tablets). Participants were confined to the clinical unit for 72 hours for drug dosing, blood sampling, and clinical assessment and were subsequently followed up as outpatients to day 28 ± 2.

A second (homologous) intravenous inoculation with ~2800 viable *P. falciparum*–infected human erythrocytes was administered on day 90 ± 7 to all participants who remained eligible (a repeat eligibility screening was performed on day 85 ± 7). Participants were administered a standard course of artemether-lumefantrine (as described above) on an individualized basis when any of the following criteria were met: parasitemia ≥ 50,000 parasites/ml, malaria clinical score > 6 and presence of parasitemia, serious adverse event related to malaria challenge, grade 3 AE related to malaria challenge and not self-resolved or relieved with concomitant medications, investigator discretion based on participant safety, or 28 days after second inoculation if the preceding criteria were not met. The end-of-study visit occurred ~28 days after artemether-lumefantrine treatment initiation.

Quantification of *P. falciparum* parasitemia and of plasma drug concentrations

Quantification of *P. falciparum* parasitemia was determined in venous blood samples by qPCR targeting the gene encoding 18*S* rRNA as described previously (*43*). Plasma drug concentrations were determined by LC-MS/MS using validated methods. Ruxolitinib was measured as described previously (*17*), with the internal standard Ruxolitinib-d9. The calibration range for ruxolitinib was 1.0 to 1000 ng/ml using 50 μl of plasma. The analytical method was precise and accurate. The descriptive statistics of the quality control (QC) samples for ruxolitinib showed that the interassay precision (% coefficient of variation) ranged from 5.3 to 8.2% ($n = 14$), whereas the interaccuracy ranged from 100.1 to 102.9% ($n = 14$) of the nominal concentrations. The QC concentrations were as follows: 3 ng/ml for low QC, 20 ng/ml for mid QC, and 750 ng/ml for high QC for ruxolitinib.

Artemether and lumefantrine, and their active metabolites (DHA and DBL), were measured as previously described (*44*). The calibration ranges were 1.0 to 1024 ng/ml using 50 μl of plasma. The QC concentrations were 4 ng/ml for low QC, 32 ng/ml for mid-QC, and 512 ng/ml for high QC. The interassay precision ranged from 3.5 to 5.9% ($n = 8$) for artemether, 4.7 to 7.7% ($n = 8$) for DHA, 4.6 to 8.5% ($n = 12$) for lumefantrine, and 5.7 to 7.3% ($n = 12$) for DBL. The interaccuracy ranged from 94.9 to 103.7% ($n = 8$) for artemether, 99.5 to 105.6% ($n = 8$) for DHA, 94.3 to 101.5% ($n = 12$) for lumefantrine, and 98.7 to 101.8% ($n = 12$) for DBL. For quality assurance, the analytical laboratory at the Australian Defence Force Malaria and Infectious Disease Institute participates in the WorldWide Antimalarial Resistance Network proficiency testing/QC program for the measurement of plasma concentrations of artemether, DHA, lumefantrine, and DBL (*45*).

Assessment of safety and tolerability

Safety and tolerability were assessed by monitoring AEs, vital signs, clinical laboratory parameters (hematology, biochemistry and urinalysis), physical examination, and electrocardiographs. A malaria clinical score was generated by grading 14 signs/symptoms frequently associated with malaria using a four-point scale (absent, 0; mild, 1; moderate, 2; severe, 3) and summing to generate a total score at each time point (maximum score possible is 42). The timing of all study assessments is indicated in the clinical trial protocol (data file S6).

Measurement of CRP

The inflammatory marker CRP was measured using a commercially available ELISA Kit (Thermo Fisher Scientific, no. KHA0031) following the manufacturer's instructions on plasma diluted 1:30,000 collected from a K2 EDTA tube. Samples were tested in duplicate according to the manufacturer's instructions. Absorbance was read at 450 nm on a Biotek PowerWave XS2 microplate reader, and concentrations were calculated from a four-parameter logistic regression of standard curve.

Phosphoflow whole-blood CyTOF

Two hundred microliters of whole blood (from Li-heparin) was stimulated with IL-6 (0.1 μg/ml; Biosciences, catalog no. BMS341) for 15 min at room temperature or left unstimulated, fixed with the Proteomic Stabilizer (PROT1, Smart Tube Inc.), and kept at −80°C. CyTOF was performed by the Human Immune Monitoring Center (HIMC) at Stanford University. Fixed samples were thawed; samples were washed with Smart Tube Thaw-Lyse buffer twice and washed with Cell Staining Buffer (CSB; Standard Biotools) once. The samples were then washed twice with perm buffer [Invitrogen 10× permeabilization buffer no. 00-8333-56, diluted to 1× in phosphate-buffered saline (PBS) from Standard Biotools]. The samples were then resuspended in 900 μl of perm buffer, and 10 μl of each Standard Biotools CellID 20plex Pd barcode was added before incubating at room temperature for 30 min. Next, the samples were centrifuged, aspirated, and washed three times by resuspension in CSB. The pellets were then resuspended in 450 μl of CSB and pooled into a single tube. After centrifugation and aspiration, the pooled sample was counted on a Bio-Rad TC20 cell counter. Surface cocktail was added at one test, 20 μl per 1 million counted cells, and stained at room temperature for 30 min. This cocktail was combined from two −80°C frozen cocktails (HIMC surface stain and Boyle surface stain), to which fresh 143Nd-CD45RA (Standard Biotools) was added. Next, the sample was washed twice by resuspension with CSB. For fixation, 4% paraformaldehyde (PFA) in PBS was added, and the sample was incubated for 10 min at room temperature before adding PBS to 10 ml, centrifugation, and aspiration. Then, 1 ml of −20°C cold methanol was added, and the sample was placed at −80°C overnight. On day 2, the sample was centrifuged, the methanol was aspirated before resuspension in 10 ml of PBS, and the centrifugation and aspiration were repeated. The sample was resuspended in 1 ml of CSB and counted using a TC20 cell counter. Intracellular cocktail was added (one test, 20 μl per 1 million counted cells) and stained at room temperature for 30 min. This cocktail was combined from two −80°C frozen cocktails (HIMC intracellular stain and Boyle intracellular stain). After staining, the sample was washed twice with CSB, centrifuged, and aspirated. The pellet was then resuspended in 2% PFA/PBS containing 250 nM Ir intercalator (Standard Biotools) and incubated for 20 min at room temperature. Cells were washed once with CSB and twice with MilliQ water. On the same day that staining was finished, cells were diluted to 0.75 M/ml in MilliQ water containing 10× diluted EQ4 normalization beads (Standard Biotools), and data were acquired by CyTOF (Helios, CyTOF model 3). Data analysis was performed using FlowJo v10 by gating on intact cells on the basis of the iridium isotopes from the intercalator and then on singlets by Ir191 versus cell length followed by cell clustering analyses. No live-dead was used because the sample was fresh, complete whole blood. For clustering analyses, data were batch-corrected using the CyCombine package (*46*), clustered using FlowSOM (*47*), and annotated by expression profiles of lineage markers on R version 4.3.3.

Parasite culture

Packed RBCs from donors were infected in vitro with the *P. falciparum* 3D7 parasite strain used to inoculate participants. Packed RBCs for parasite culture were acquired from the Australian Red Cross. pRBCs were cultured at 5% hematocrit in RPMI 1640 supplemented with AlbuMAX II (0.25%) and heat-inactivated human serum (5%). Cultures were incubated at 37°C in a 1% O_2, 5% CO_2, and 94% N_2 gas mixture. Culture medium was replaced daily, and parasite stage/parasitemia was monitored by Giemsa-stained blood smears. Parasites were synchronized with 5% sorbitol after each round of in vitro invasion. pRBCs were grown to 15% parasitemia and purified from uRBCs and early-stage pRBCs by magnet separation to enrich mature trophozoite–stage pRBCs, and a single batch of parasites was used for all stimulations. Purified pRBCs (>95% purity) were stored at −80°C after addition of a glycerolyte cryopreservant. For use in in vitro stimulations, glycerolyte-preserved parasites or control uRBCs were thawed by dropwise addition of malaria thawing solution (MTS: 0.6% NaCl in H_2O) and incubated at room temperature for 10 min. Parasites were washed in MTS/PBS three times with decreasing solution ratios (1:0, 1:1, and 0:1). After thaw, parasites were intact late-stage trophozoites.

PBMC parasite stimulation and Luminex

PBMCs and plasma were isolated by density centrifugation with Ficoll gradient separation from whole blood collected in lithium heparin tubes (BD Biosciences). Isolated PBMCs were cryopreserved in 10% dimethyl sulfoxide/fetal bovine serum. PBMCs were thawed in RPMI 1640 (Gibco) containing 10% fetal calf serum and 0.02% Benzonase. A total of 2.5×10^5 PBMCs were stimulated with 7.5×10^5 3D7 strain parasite–infected RBCs or uRBCs (1 PBMC:3 pRBC or uRBC) in 96-well U-bottom plates (*9*). Culture supernatants were collected after 72 hours. IFN-γ and IL-10 were measured by Luminex with human 48 plex kits performed by the Immunoassay Team at the HIMC at Stanford University. Kits were purchased from EMD Millipore Corporation (Milliplex HCYTA-60K-PX48). The assay setup followed the recommended protocol. Briefly, samples were diluted 3-fold for panels 1 and 2 or 10-fold for panel 3. A total of 25 μl of the diluted sample was mixed with antibody-linked magnetic beads in a 96-well plate and incubated overnight at 4°C with shaking. Cold and room temperature incubation steps were performed on an orbital shaker at 500 to 600 rpm. Plates were washed twice with wash buffer in a BioTek ELx405 washer (BioTek Instruments). After a 1-hour incubation at room temperature with biotinylated detection antibody, streptavidin-phycoerythrin was added for 30 min with shaking. These reagents were used as supplied by the manufacturer without dilution. Plates were washed as described above, and PBS was added to wells for reading in the Luminex FlexMap3D Instrument with a lower bound of 50 beads per sample per cytokine. Each sample was measured with single replicates. Custom Assay Chex control beads were purchased and added to all wells (Radix BioSolutions). Wells with a bead count below 50 were flagged, and data with a bead count below 20 were excluded.

NULISA inflammation panel

This assay was performed by the HIMC at Stanford University on plasma collected from lithium-heparin tubes. Samples were run on the NULISA Inflammation panel (Alamar Biosciences, Fremont, California), a multiplexed proximity ligation assay targeting 248 to 250 inflammation-associated proteins (250 analytes were for all first infection samples and 248 analytes for the second infection samples). The assay was processed automatically in the ARGO HT system (Alamar Biosciences). A total of 25 μl of each sample was loaded on the sample plate, along with three sample controls, four negative controls, and three interplate controls. After completion of the automated run, next-generation sequencing (Illumina) was performed on the pooled library. Data were generated using Alamar Command Center and NULISA Analysis Software by normalization to internal controls and interplate controls. Then, data were rescaled using $\log_2$ transformation. These steps produced an output in NULISA Protein Quantification units. The participant who tested positive for COVID-19 after the second infection, requiring early treatment with artemether-lumefantrine, was excluded from the analysis of the re-inoculation time points.

Statistical analysis

The number of AEs per participant was compared between treatment groups at each study phase using a Wilcoxon rank sum test. To further assess clinical symptoms during the posttreatment 72-hour confinement period after the first inoculation, as a post hoc analysis, the sum of the malaria clinical score at each time point assessed was calculated. Spearman's correlation (conducted using Stata v18) was used to evaluate the association between the sum of the malaria clinical score, peak parasitemia, and peak CRP.

Plasma artemether, DHA, lumefantrine, DBL, and ruxolitinib concentration time data were analyzed by noncompartmental methods using PKanalix (version 2023R1). Differences in PK parameters between placebo and ruxolitinib groups were tested using an unpaired two-sample *t* test or Wilcoxon test.

The PRR_{48} and $PCt_{1/2}$ were estimated using the slope of the optimal fit for the log-linear relationship of the parasitemia decay (*18*). Differences between treatment groups in parasite clearance parameters after first inoculation were assessed using an omnibus test. The analysis was conducted using R version 4.1.3.

The parasite growth rate and associated PMR_{48} were calculated by applying a sine-wave growth model to the parasitemia data (*48*). Mixed-effects models were used to obtain parameter estimates overall after the first inoculation and for each treatment group after the second inoculation. Changes in PMR_{48} between inoculation phases were assessed by applying a mixed-effect segmented regression sine wave model with a treatment group–by-time interaction after the second inoculation. Full model specifications are provided in Supplementary Materials and Methods. Time to parasitemia after the second inoculation was compared between groups using a Fisher's exact test. All PMR_{48} analyses were conducted using Stata version 18.

The change in immune responses over time from either the inoculation or the treatment time point was assessed using log-linear mixed-effects models with restricted maximum likelihood (REML) estimation, incorporating a random intercept at the participant level. For changes between the first inoculation and treatment time point, only time point was added as a fixed effect. Treatment, time point, and their interaction were included as fixed effects to evaluate how the response differed between treatment groups and how the change in response over time differed between treatment groups. The change over time for the ruxolitinib group was assessed using contrasts. Residual bootstrapping for linear mixed-effects models at 5000 iterations was applied to account for potential deviations from normality in the residuals, ensuring robust and reliable estimates.

FDR was controlled using the Benjamini-Hochberg method, grouped per time point comparison and all model fixed effects.

A segmented regression approach was used to assess changes in inflammatory and immune responses from the inoculation to treatment time point and how these changes differed between first and second infection (phase) and between treatment groups. Log-linear mixed-effect models included time point, treatment, phase, and a phase-by-day interaction as fixed effects, with participant-level random effect and REML estimation. Residual bootstrapping and multiple comparisons adjustment were applied as previously indicated. Full model specifications are provided in Supplementary Materials and Methods. Immunology analysis was conducted using R version 4.3.3.

Supplementary Materials

The PDF file includes:
Materials and Methods
Figs. S1 to S3
Tables S1 to S14
Legends for data files S1 to S6

Other Supplementary Material for this manuscript includes the following:
Data files S1 to S6
MDAR Reproducibility Checklist

REFERENCES AND NOTES

1. World Health Organization, *World Malaria Report 2024* (World Health Organization, 2024).
2. A. Dondorp, F. Nosten, K. Stepniewska, N. Day, N. White, South East Asian Quinine Artesunate Malaria Trial (SEAQUAMAT) group, Artesunate versus quinine for treatment of severe falciparum malaria: A randomised trial. *Lancet* **366**, 717–725 (2005).
3. A. Olotu, G. Fegan, J. Wambua, G. Nyangweso, A. Leach, M. Lievens, D. C. Kaslow, P. Njuguna, K. Marsh, P. Bejon, Seven-year efficacy of RTS, S/AS01 malaria vaccine among young African children. *N. Engl. J. Med.* **374**, 2519–2529 (2016).
4. S. Rts, Efficacy and safety of RTS, S/AS01 malaria vaccine with or without a booster dose in infants and children in Africa: Final results of a phase 3, individually randomised, controlled trial. *Lancet* **386**, 31–45 (2015).
5. M. S. Datoo, A. Dicko, H. Tinto, J.-B. Ouédraogo, M. Hamaluba, A. Olotu, E. Beaumont, F. R. Lopez, H. M. Natama, S. Weston, M. Chemba, Y. D. Compaore, D. Issiaka, D. Salou, A. M. Some, S. Omenda, A. Lawrie, P. Bejon, H. Rao, D. Chandramohan, R. Roberts, S. Bharati, L. Stockdale, S. Gairola, B. M. Greenwood, K. J. Ewer, J. Bradley, P. S. Kulkarni, U. Shaligram, A. V. S. Hill, R21/Matrix-M Phase 3 Trial Group, Safety and efficacy of malaria vaccine candidate R21/Matrix-M in African children: A multicentre, double-blind, randomised, phase 3 trial. *Lancet* **403**, 533–544 (2024).
6. M. J. Boyle, C. R. Engwerda, P. Jagannathan, The impact of *Plasmodium*-driven immunoregulatory networks on immunity to malaria. *Nat. Rev. Immunol.* **24**, 637–653 (2024).
7. A. Haque, S. E. Best, M. M. de Oca, K. R. James, A. Ammerdorffer, C. L. Edwards, F. de Labastida Rivera, F. H. Amante, P. T. Bunn, M. Sheel, I. Sebina, M. Koyama, A. Varelias, P. J. Hertzog, U. Kalinke, S. Y. Gun, L. Rénia, C. Ruedl, K. P. A. Mac Donald, G. R. Hill, C. R. Engwerda, Type I IFN signaling in $CD8^-$ DCs impairs Th1-dependent malaria immunity. *J. Clin. Invest.* **124**, 2483–2496 (2014).
8. C. L. Edwards, S. S. Ng, F. de Labastida Rivera, D. Corvino, J. A. Engel, M. M. de Oca, L. Bukali, T. C. Frame, P. T. Bunn, S. B. Chauhan, S. S. Singh, Y. Wang, J. Na, F. H. Amante, J. R. Loughland, M. S. Soon, N. Waddell, P. Mukhopadhay, L. T. Koufariotis, R. L. Johnston, J. S. Lee, R. Kuns, P. Zhang, M. J. Boyle, G. R. Hill, J. S. McCarthy, R. Kumar, C. R. Engwerda, IL-10-producing Th1 cells possess a distinct molecular signature in malaria. *J. Clin. Invest.* **133**, e153733 (2023).
9. M. M. de Oca, R. Kumar, F. de Labastida Rivera, F. H. Amante, M. Sheel, R. J. Faleiro, P. T. Bunn, S. E. Best, L. Beattie, S. S. Ng, C. L. Edwards, G. M. Boyle, R. N. Price, N. M. Anstey, J. R. Loughland, J. Burel, D. L. Doolan, A. Haque, J. S. McCarthy, C. R. Engwerda, Type I interferons regulate immune responses in humans with blood-stage *Plasmodium falciparum* infection. *Cell Rep.* **17**, 399–412 (2016).
10. Y. Wang, F. De Labastida Rivera, C. L. Edwards, T. C. Frame, J. A. Engel, L. Bukali, J. Na, S. S. Ng, D. Corvino, M. M. de Oca, P. T. Bunn, M. S. Soon, D. Andrew, J. R. Loughland, J. Zhang, F. H. Amante, B. E. Barber, J. S. McCarthy, J. A. Lopez, M. J. Boyle, C. R. Engwerda, STING activation promotes autologous type I interferon–dependent development of type 1 regulatory T cells during malaria. *J. Clin. Invest.* **133**, e169417 (2023).
11. M. Walther, J. Woodruff, F. Edele, D. Jeffries, J. E. Tongren, E. King, L. Andrews, P. Bejon, S. C. Gilbert, J. B. De Souza, R. Sinden, A. V. S. Hill, E. M. Riley, Innate immune responses to human malaria: Heterogeneous cytokine responses to blood-stage *Plasmodium falciparum* correlate with parasitological and clinical outcomes. *J. Immunol.* **177**, 5736–5745 (2006).
12. P. Jagannathan, I. Eccles-James, K. Bowen, F. Nankya, A. Auma, S. Wamala, C. Ebusu, M. K. Muhindo, E. Arinaitwe, J. Briggs, B. Greenhouse, J. W. Tappero, M. R. Kamya, G. Dorsey, M. E. Feeney, IFNγ/IL-10 co-producing cells dominate the CD4 response to malaria in highly exposed children. *PLOS Pathog.* **10**, e1003864 (2014).
13. M. Montes de Oca, M. F. Good, J. S. McCarthy, C. R. Engwerda, The impact of established immunoregulatory networks on vaccine efficacy and the development of immunity to malaria. *J. Immunol.* **197**, 4518–4526 (2016).
14. L. C. Platanias, Mechanisms of type-I-and type-II-interferon-mediated signalling. *Nat. Rev. Immunol.* **5**, 375–386 (2005).
15. M.-L. Frémond, M. P. Rodero, N. Jeremiah, A. Belot, E. Jeziorski, D. Duffy, D. Bessis, G. Cros, G. I. Rice, B. Charbit, A. Hulin, N. Khoudour, C. M. Caballero, C. Bodemer, M. Fabre, L. Berteloot, M. le Bourgeois, P. Reix, T. Walzer, D. Moshous, S. Blanche, A. Fischer, B. Bader-Meunier, F. Rieux-Laucat, Y. J. Crow, B. Neven, Efficacy of the Janus kinase 1/2 inhibitor ruxolitinib in the treatment of vasculopathy associated with TMEM173-activating mutations in 3 children. *J. Allergy Clin. Immunol.* **138**, 1752–1755 (2016).
16. R. Kumar, P. T. Bunn, S. S. Singh, S. S. Ng, M. M. de Oca, F. De Labastida Rivera, S. B. Chauhan, N. Singh, R. J. Faleiro, C. L. Edwards, T. C. M. Frame, M. Sheel, R. J. Austin, S. W. Lane, T. Bald, M. J. Smyth, G. R. Hill, S. E. Best, A. Haque, D. Corvino, N. Waddell, L. Koufariotis, P. Mukhopadhay, M. Rai, J. Chakravarty, O. P. Singh, D. Sacks, S. Nylen, J. Uzonna, S. Sundar, C. R. Engwerda, Type I interferons suppress anti-parasitic immunity and can be targeted to improve treatment of visceral leishmaniasis. *Cell Rep.* **30**, 2512–2525.e9 (2020).
17. M. F. Chughlay, K. I. Barnes, M. E. Gaaloul, N. Abla, J. J. Möhrle, P. Griffin, P. van Giersbergen, S. E. Reuter, H. B. Schultz, A. Kress, P. Tapley, R. A. Webster, T. Wells, J. S. McCarthy, B. E. Barber, L. Marquart, M. J. Boyle, C. R. Engwerda, S. Chalon, Safety, tolerability, pharmacokinetics, and pharmacodynamics of coadministered ruxolitinib and artemether-lumefantrine in healthy adults. *Antimicrob. Agents Chemother.* **66**, e0158421 (2022).
18. L. Marquart, M. Baker, P. O'Rourke, J. S. McCarthy, Evaluating the pharmacodynamic effect of antimalarial drugs in clinical trials by quantitative PCR. *Antimicrob. Agents Chemother.* **59**, 4249–4259 (2015).
19. S. D. Woolley, L. Marquart, J. Woodford, S. Chalon, J. J. Moehrle, J. S. McCarthy, B. E. Barber, Haematological response in experimental human *Plasmodium falciparum* and *Plasmodium vivax* malaria. *Malar. J.* **20**, 1–13 (2021).
20. J. Woodford, T. W. Yeo, K. A. Piera, K. Butler, J. B. Weinberg, J. S. McCarthy, N. M. Anstey, B. E. Barber, Early endothelial activation precedes glycocalyx degradation and microvascular dysfunction in experimentally induced *Plasmodium falciparum* and *Plasmodium vivax* infection. *Infect. Immun.* **88**, 10.1128/IAI.00895-19 (2020).
21. A. N. Abd-Rahman, D. Kaschek, A. Kümmel, R. Webster, A. J. Potter, A. Odedra, S. D. Woolley, S. Llewellyn, L. Webb, L. Marquart, S. Chalon, M. Gaaloul, J. McCarthy, J. J. Möehrle, B. Barber, Characterizing the pharmacological interaction of the antimalarial combination artefenomel-piperaquine in healthy volunteers with induced blood-stage *Plasmodium falciparum* to predict efficacy in patients with malaria. *BMC Med.* **22**, 563 (2024).
22. M. F. Chughlay, S. Akakpo, A. Odedra, K. Csermak-Renner, E. Djeriou, C. Winnips, D. Leboulleux, A. H. Gaur, G. D. Shanks, J. McCarthy, S. Chalon, Liver enzyme elevations in *Plasmodium falciparum* volunteer infection studies: Findings and recommendations. *Am. J. Trop. Med. Hyg.* **103**, 378–393 (2020).
23. S. D. Woolley, M. J. Grigg, L. Marquart, J. S. E. Gower, K. Piera, A. S. Nair, F. M. Amante, G. S. Rajahram, T. William, D. M. Frazer, S. Chalon, J. S. McCarthy, N. M. Anstey, B. E. Barber, Longitudinal changes in iron homeostasis in human experimental and clinical malaria. *EBioMedicine* **105**, 105189 (2024).
24. P. Wilairatana, W. Mala, G. D. J. Milanez, F. R. Masangkay, K. U. Kotepui, M. Kotepui, Increased interleukin-6 levels associated with malaria infection and disease severity: A systematic review and meta-analysis. *Sci. Rep.* **12**, 5982 (2022).
25. T. W. Yeo, D. A. Lampah, R. Gitawati, E. Tjitra, E. Kenangalem, K. Piera, R. N. Price, S. B. Duffull, D. S. Celermajer, N. M. Anstey, Angiopoietin-2 is associated with decreased endothelial nitric oxide and poor clinical outcome in severe falciparum malaria. *Proc. Natl. Acad. Sci. U.S.A.* **105**, 17097–17102 (2008).
26. S. Adukpo, K. A. Kusi, M. F. Ofori, J. K. A. Tetteh, D. Amoako-Sakyi, B. Q. Goka, G. O. Adjei, D. A. Edoh, B. D. Akanmori, B. A. Gyan, D. Dodoo, High plasma levels of soluble intercellular adhesion molecule (ICAM)-1 are associated with cerebral malaria. *PLOS ONE* **8**, e84181 (2013).
27. T. W. Yeo, J. B. Weinberg, D. A. Lampah, E. Kenangalem, P. Bush, Y. Chen, R. N. Price, S. Young, H. Y. Zhang, D. Millington, Glycocalyx breakdown is associated with severe disease and fatal outcome in *Plasmodium falciparum* malaria. *Clin. Infect. Dis.* **69**, 1712–1720 (2019).

28. L. M. Randall, F. H. Amante, Y. Zhou, A. C. Stanley, A. Haque, F. Rivera, K. Pfeffer, S. Scheu, G. R. Hill, K. Tamada, C. R. Engwerda, Cutting edge: Selective blockade of LIGHT-lymphotoxin β receptor signaling protects mice from experimental cerebral malaria caused by *Plasmodium berghei* ANKA. *J. Immunol.* **181**, 7458–7462 (2008).
29. T. Zhao, Z. Su, Y. Li, X. Zhang, Q. You, Chitinase-3 like-protein-1 function and its role in diseases. *Signal Transduct. Target. Ther.* **5**, 201 (2020).
30. J. Wang, C.-Y. Chang, X. Yang, F. Zhou, J. Liu, Z. Feng, W. Hu, Leukemia inhibitory factor, a double-edged sword with therapeutic implications in human diseases. *Mol. Ther.* **31**, 331–343 (2023).
31. L. Bukali, D. Oyong, F. de Labastida Rivera, J. A. Engel, R. Webster, F. Amante, M. D. Leipold, G. Oberoser, H. Maecker, J. McCarthy, B. E. Barber, M. J. Boyle, C. Engwerda, Transient JAK/STAT inhibition by ruxolitinib modulates malaria-specific $CD4^+$ T cell responses and enhances recall immunity in volunteers experimentally infected with *Plasmodium falciparum*. medRxiv 25325416 [Preprint] (2025). https://doi.org/10.1101/2025.04.09.25325416.
32. U. Fiedler, Y. Reiss, M. Scharpfenecker, V. Grunow, S. Koidl, G. Thurston, N. W. Gale, M. Witzenrath, S. Rosseau, N. Suttorp, A. Sobke, M. Herrmann, K. T. Preissner, P. Vajkoczy, H. G. Augustin, Angiopoietin-2 sensitizes endothelial cells to TNF-α and has a crucial role in the induction of inflammation. *Nat. Med.* **12**, 235–239 (2006).
33. G. D. H. Turner, H. Morrison, M. Jones, T. M. E. Davis, S. Looareesuwan, I. D. Buley, K. C. Gatter, C. I. Newbold, S. Pukritayakamee, B. Nagachinta, N. J. White, A. R. Berendt, An immunohistochemical study of the pathology of fatal malaria: Evidence for widespread endothelial activation and a potential role for intercellular adhesion molecule-1 in cerebral sequestration. *Am. J. Pathol.* **145**, 1057–1069 (1994).
34. A. L. Conroy, S. J. Glover, M. Hawkes, L. K. Erdman, K. B. Seydel, T. E. Taylor, M. E. Molyneux, K. C. Kain, Angiopoietin-2 levels are associated with retinopathy and predict mortality in Malawian children with cerebral malaria: A retrospective case-control study. *Crit. Care Med.* **40**, 952–959 (2012).
35. B. E. Barber, M. J. Grigg, K. Piera, T. William, M. J. Boyle, T. W. Yeo, N. M. Anstey, Effects of aging on parasite biomass, inflammation, endothelial activation and microvascular dysfunction in *Plasmodium knowlesi* and *P. falciparum* malaria. *J. Infect. Dis.* **215**, 1908–1917 (2017).
36. J. R. Poespoprodjo, N. M. Douglas, D. Ansong, S. Kho, N. M. Anstey, Malaria. *Lancet* **402**, 2328–2345 (2023).
37. M. Febvre-James, V. Lecureur, O. Fardel, Potent repression of C-reactive protein (CRP) expression by the JAK1/2 inhibitor ruxolitinib in inflammatory human hepatocytes. *Inflamm. Res.* **69**, 51–62 (2020).
38. F. Prenen, L. Vandermosten, S. Knoops, E. Pollenus, H. Possemiers, P. Dagneau de Richecour, G. Caratti, C. Cawthorne, S. Vettorazzi, Y. Cranshoff, D. Schols, S. Claes, C. M. Deroose, U. Himmelreich, J. Tuckermann, P. van den Steen, JAK/STAT inhibition protects glucocorticoid receptor knockout mice from lethal malaria-induced hypoglycemia and hyperinflammation. *EMBO Mol. Med.* **17**, 2040–2070 (2025).
39. S. Verstovsek, H. Kantarjian, R. A. Mesa, A. D. Pardanani, J. Cortes-Franco, D. A. Thomas, Z. Estrov, J. S. Fridman, E. C. Bradley, S. Erickson-Viitanen, K. Vaddi, R. Levy, A. Tefferi, Safety and efficacy of INCB018424, a JAK1 and JAK2 inhibitor, in myelofibrosis. *N. Engl. J. Med.* **363**, 1117–1127 (2010).
40. L. Piatti, A. Batzilla, F. Nakaki, H. Fleckenstein, F. Korbmacher, R. K. Long, D. Schraivogel, J. A. Hawkins, T. Romero-Uruñuela, B. López-Gutiérrez, S. Sanz Sender, Y. Schwab, L. M. Steinmetz, J. Sharpe, M. Bernabeu, *Plasmodium falciparum* egress disrupts endothelial junctions and activates JAK-STAT signaling in a microvascular 3D blood-brain barrier model. *Nat. Commun.* **16**, 7262 (2025).
41. I. Comerford, Y. Harata-Lee, M. D. Bunting, C. Gregor, E. E. Kara, S. R. McColl, A myriad of functions and complex regulation of the CCR7/CCL19/CCL21 chemokine axis in the adaptive immune system. *Cytokine Growth Factor Rev.* **24**, 269–283 (2013).
42. T. Francis, On the doctrine of original antigenic sin. *Proc. Am. Philos. Soc.* **104**, 572–578 (1960).
43. C. Y. Wang, E. L. Ballard, Z. Pava, L. Marquart, J. Gaydon, S. C. Murphy, D. Whiley, P. O'Rourke, J. S. McCarthy, Analytical validation of a real-time hydrolysis probe PCR assay for quantifying *Plasmodium falciparum* parasites in experimentally infected human adults. *Malar. J.* **20**, 1–8 (2021).
44. N. C. Phong, M. Chavchich, H. H. Quang, N. N. San, G. W. Birrell, I. Chuang, N. J. Martin, N. D. Manh, M. D. Edstein, Susceptibility of *Plasmodium falciparum* to artemisinins and *Plasmodium vivax* to chloroquine in Phuoc Chien Commune, Ninh Thuan Province, south-central Vietnam. *Malar. J.* **18**, 10 (2019).
45. C. Lourens, N. Lindegardh, K. I. Barnes, P. J. Guerin, C. H. Sibley, N. J. White, J. Tarning, Benefits of a pharmacology antimalarial reference standard and proficiency testing program provided by the Worldwide Antimalarial Resistance Network (WWARN). *Antimicrob. Agents Chemother.* **58**, 3889–3894 (2014).
46. C. B. Pedersen, S. H. Dam, M. B. Barnkob, M. D. Leipold, N. Purroy, L. Z. Rassenti, T. J. Kipps, J. Nguyen, J. A. Lederer, S. H. Gohil, C. J. Wu, L. R. Olsen, cyCombine allows for robust integration of single-cell cytometry datasets within and across technologies. *Nat. Commun.* **13**, 1698 (2022).
47. S. Van Gassen, B. Callebaut, M. J. Van Helden, B. N. Lambrecht, P. Demeester, T. Dhaene, Y. Saeys, FlowSOM: Using self-organizing maps for visualization and interpretation of cytometry data. *Cytometry A* **87**, 636–645 (2015).
48. L. F. Wockner, I. Hoffmann, L. Webb, B. Mordmüller, S. C. Murphy, J. G. Kublin, P. O'rourke, J. S. McCarthy, L. Marquart, Growth rate of *Plasmodium falciparum*: Analysis of parasite growth data from malaria volunteer infection studies. *J. Infect. Dis.* **221**, 963–972 (2020).

Acknowledgments: We thank the volunteers who participated in the clinical trial, staff at the University of Sunshine Coast clinical trial site, staff at the Queensland Paediatric Infectious Diseases Laboratory (QPID) for conducting the malaria PCR assays, members of the Stanford HIMC for technical assistance, and K. Van Breda for technical assistance in the analysis of drug concentrations. **Funding:** This study was funded by the Australian National Health and Medical Research Council (NHMRC) Ideas Grant to B.E.B. and M.J.B. (GNT2002957). B.E.B. and J.S.M. are supported by NHMRC Investigator Grants (2016792 and 2016396, respectively); M.J.B. is supported by a Snow Medical Fellowship (2022/SF167) and CSL Centenary Fellowship. The funders had no role in the design, conduct, analysis, or reporting of the clinical trial. The Australian Defence Organisation provided in-kind contribution to the measurement of plasma ruxolitinib, artemether, lumefantrine, and their active metabolite concentrations by LC-MS/MS. Work in the Stanford HIMC was supported by the Gates Foundation (INV-008378). The conclusions and opinions expressed in this work are those of the author(s) alone and shall not be attributed to the Foundation. Under the grant conditions of the Gates Foundation, a Creative Commons Attribution 4.0 License has been assigned to the author-accepted version of the manuscript. **Author contributions:** C.R.E., M.J.B., J.S.M., B.E.B., S.C., J.J.M., and T.N.C.W. conceptualized the study. L.B., J.E., M.S.F.S., T.F., J.H., M.N., N.L.D., J.R.L., A.J.P., and R. Webster optimized protocols. R.M., D.W.A., L.B., F.d.L.R., J.E., M.S.F.S., T.F., J.H., M.N., N.L.D., and J.R.L. generated data for immunology end points. T.N., Y.R.-H, S.M.-A., N. Sigal, K.F., M.L., G.O., and H.M. generated Luminex, NULISA, and pCyTOF data. G.W.B. and M.D.E. generated drug concentration data. D.A.O., R.M., F.d.L.R., C.R.E., M.J.B., B.E.B., A.N.A.-R., and S.L. analyzed data. N. Sahai, I.L., E.U., J.G., J.P., and F.A. coordinated the clinical study and participant sampling. D.W.A., F.d.L.R., M.L., G.O., H.M., S.M., and R. Webster provided project management. R. Woo performed data management. C.R.E., M.J.B., B.E.B., M.L., G.O., H.M., and R. Webster provided supervision. D.A.O., C.R.E., M.J.B., B.E.B., and A.J.P. wrote the first draft of the manuscript with feedback from all authors. M.J.B., C.R.E., B.E.B., T.N.C.W., S.C., and J.J.M. provided funding. **Competing interests:** M.J.B. (2025), B.E.B. (2023–2025), and J.S.M. (2023–2025) provided paid consulting to Merck (Rahway, NJ, USA). B.E.B. received institutional funding from Medicines for Malaria Venture (Geneva, Switzerland) to support the conduct of malaria volunteer infection studies. J.J.M. provided paid consulting to Sumaya Biotech (Heidelberg Germany), Institut für Tropenmedizin (University of Tübingen, Germany), and RIGHT foundation (Seoul, Korea) in 2025. H.M. has provided paid consulting to Curiox Biosystems (Woburn, MA, USA) since 2022 and has been on the scientific advisory board for Cytek Biosciences (Fremont, CA, USA) since 2016. All other authors declare that they have no competing interests. **Data and materials availability:** All data associated with this study are present in the paper or the Supplementary Materials. NULISA, Luminex, and pCyTOF whole blood data are publicly available at DOIs 10.5281/zenodo.15080321, 10.5281/zenodo.14861648, and 10.5281/zenodo.14872946. Analysis code can be found at DOI 10.5281/zenodo.17222037.

Submitted 8 July 2025
Accepted 17 October 2025
Published 26 November 2025
10.1126/scitranslmed.aea2531

Science Translational Medicine

Adjunctive ruxolitinib attenuates inflammation and enhances immunity in volunteers experimentally infected with *Plasmodium falciparum*

Rebecca Webster, Damian A. Oyong, Stacey Llewellyn, Azrin N. Abd-Rahman, Adam J. Potter, Reena Mukhiya, Nischal Sahai, Indika Leelasena, Eniko Ujvary, Sue Mathison, Dean W. Andrew, Luzia Bukali, Fabian de Labastida Rivera, Jessica Engel, Megan S. F. Soon, Teija Frame, Julianne Hamelink, Mayimuna Nalubega, Nicholas L. Dooley, Jessica R. Loughland, Tran Nguyen, Yael Rosenberg-Hasson, Sofia Maysel-Auslender, Natalia Sigal, Kira Foygel, Jeremy Gower, Jenny Peters, Ria Woo, Fiona Amante, Timothy N. C. Wells, Stephan Chalon, Joerg J. Moehrle, James S. McCarthy, Geoffrey W. Birrell, Michael D. Edstein, Michael Leipold, Gerlinde Obermoser, Holden Maecker, Christian R. Engwerda, Bridget E. Barber, and Michelle J. Boyle

Sci. Transl. Med. **17** (826), eaea2531. DOI: 10.1126/scitranslmed.aea2531

Editor's summary

Malaria infection elicits inflammatory responses that impede development of protective antimalaria immunity, leaving individuals more susceptible to subsequent infections. Here, Webster *et al.* asked whether inhibiting this inflammatory response with an adjunctive therapy could boost elicitation of immune memory. The authors inoculated malaria-naïve volunteers with *Plasmodium falciparum* and treated them with the JAK1/2 inhibitor ruxolitinib in addition to antimalarials. The authors found that ruxolitinib attenuated inflammation after the first challenge, reducing phosphorylation of STAT proteins in immune cells as expected. Moreover, upon a second challenge with *P. falciparum*, the participants who had previously received adjunctive ruxolitinib had signatures of enhanced immune memory. These data suggest that ruxolitinib, a well-tolerated and clinically used drug, could be an effective addition to the malaria therapeutic toolkit. —Courtney Malo

Science Translational Medicine (ISSN 1946-6242) is published by the American Association for the Advancement of Science. 1200 New York Avenue NW, Washington, DC 20005. The title *Science Translational Medicine* is a registered trademark of AAAS.